catalysts

MDPI

Review

A Review on Properties and Environmental Applications of Graphene and Its Derivative-Based Composites

Sanjay Kumar [1], Himanshi [2], Jyoti Prakash [2], Ankit Verma [3], Suman [4], Rohit Jasrotia [2,5,*], Abhishek Kandwal [2], Ritesh Verma [6], Sachin Kumar Godara [7], M. A. Majeed Khan [8], Saad M. Alshehri [9] and Jahangeer Ahmed [9,*]

1 School of Advanced Chemical Sciences, Shoolini University, Bajhol, Solan 173229, Himachal Pradesh, India
2 School of Physics and Materials Science, Shoolini University, Bajhol, Solan 173229, Himachal Pradesh, India
3 Faculty of Science and Technology, ICFAI University, Baddi 174103, Himachal Pradesh, India
4 School of Basic and Applied Sciences, Maharaja Agrasen University, Baddi 174103, Himachal Pradesh, India
5 Himalayan Centre of Excellence in Nanotechnology, Shoolini University, Bajhol, Solan 173229, Himachal Pradesh, India
6 Department of Physics, Amity University, Gurgaon 122413, Haryana, India
7 Department of Apparel and Textile Technology, Guru Nanak Dev University, Amritsar 143005, Punjab, India
8 King Abdullah Institute for Nanotechnology, King Saud University, Riyadh 11451, Saudi Arabia
9 Department of Chemistry, College of Science, King Saud University, Riyadh 11451, Saudi Arabia
* Correspondence: rohitjasrotia@shooliniuniversity.com (R.J.); jahmed@ksu.edu.sa (J.A.); Tel.: +91-914-988-6631 (R.J.); +966-58-146-6291 (J.A.)

Abstract: Graphene-based materials have gained a lot of scientific interest in the research era of modern technology, which can be quite flexible. Graphene has become popular as a potential material for the manufacture of a wide range of technologies due to its remarkable electrical, mechanical, and optical traits. Due to these excellent characteristics, the derivatives of graphene can be functionalized in various applications including environmental, medical, electronic, defence applications, and many more. In this review paper, we discussed the different synthesis methods for the extraction of graphene and its derivatives. The different traits of graphene and its derivatives such as structural, mechanical, and optical were also discussed. An extensive literature review on the application of graphene-based composites is presented in this work. We also outlined graphene's potential in the realm of environmental purification through different techniques such as filtration, adsorption, and photocatalysis. Lastly, the challenges and opportunities of graphene and its derivatives for advanced environmental applications were reported.

Keywords: graphene; derivatives; photocatalysis; adsorption; environmental pollution

Citation: Kumar, S.; Himanshi; Prakash, J.; Verma, A.; Suman; Jasrotia, R.; Kandwal, A.; Verma, R.; Kumar Godara, S.; Khan, M.A.M.; et al. A Review on Properties and Environmental Applications of Graphene and Its Derivative-Based Composites. *Catalysts* **2023**, *13*, 111. https://doi.org/10.3390/catal13010111

Academic Editors: Xinjiang Hu, Xiaofei Tan, Jiang Li, Chenyang Li and David Sebastián

Received: 3 November 2022
Revised: 16 December 2022
Accepted: 28 December 2022
Published: 4 January 2023

1. Introduction

Graphene is a form of elemental carbon that has recently gained a lot of attention due to its unique properties. It consists of a single layer of carbon atoms that are organized in a pattern similar to that of a honeycomb. The first team to successfully produce graphene was led by Andre Geim and Konstantin Novoselov in the year 2004. Despite this, they acknowledged Hanns Peter Bohem and other laboratory researchers who carried out tests comparing graphene with thin graphite flakes for this finding. Thus, in 1986, Hanns Peter Bohem was the first person to use the term "graphene" [1]. Even before this, many scientists and researchers had already conducted research on the lamellae of graphite. Schafhaeutl found that graphite flaked off in the presence of sulfuric and nitric acid in the 1840s, and after that in 1859, Benjamin Brodie found that graphite oxide that had been heated and cooled had a lamellar structure [2–4]. Professors Geim and Novorelov won the Novel Prize in 2010 for their contributions to the field of physics, which helped to bring graphene to public attention [5]. The bond length between the C-C atoms in graphene is 0.142 nanometres, and graphene exhibits sp^2 hybridization. Graphene has one layer of atomic thickness, whereas one square meter of graphene weighs about 0.77 milligrams,

which makes it the thinnest and lightest substance yet discovered. It also shows high conductance of heat and electricity [6]. The thermal and electrical conductivity of graphene is found to be about 5300 W/mk [7] and 10^6 S/m, which is the highest recorded in any solid [8]. It is the strongest material ever discovered and is comparable to diamond [9]. Additionally, it demonstrates consistent absorption across the visible and near-infrared light spectrums along with impermeable behaviour to gases [10–13]. Graphene's high mechanical strength allows it to be used in the strengthening of other materials. It can drastically increase the physical strength of various plastics, metals, and other composite materials. Graphene-based materials can be used in aerospace, building materials, super cars, and airplanes. The thermal conductivity of graphene makes it useful for heat sink and cooling applications. In addition, graphene's high surface-to-volume ratio allows for its use in energy storage devices, sensing applications, medical applications, and flexible solar panels. Not only graphene but also its derivatives show promising properties for potential applications.

The objective of writing this review article was to provide comprehensive literature on the various synthesis approaches for the extraction of graphene and its derivatives. In addition, the structural, optical, and mechanical traits of graphene-based materials were reported. We also addressed the graphene potential for the remediation of environmental pollution via filtration, adsorption, and photocatalysis techniques. Finally, the shortcomings and future scope for the use of graphene and its derivatives were conferred in this review paper.

1.1. Major Derivatives of Graphene

There are three major derivatives of graphene: graphane, fluorographene, and graphene oxide. Figure 1 shows the graphical representation of graphane, fluorographene, and graphene oxide with some other derivatives of graphene such as graphite, carbon nanotubes, and fullerenes. All these graphene derivatives are vastly different from one another because of their distinctive properties. Pure graphene is one atomic layer thick, which gives rise to some interesting properties such as high electrical conductivity, excellent physiochemical properties, high thermal conductivity, and unique optical properties. The derivative of graphene shows a different set of properties from pure graphene because they vary in structure and chemical composition. For example, graphite, which is made up of many layers of graphene, shows a brittle nature as opposed to pure graphene. In graphene, carbon atoms are bounded together by three sigma bonds and have a single pi bond that is oriented out of the graphene plane, but in graphite, each atom is bounded by three covalent bonds and is left with a free electron. In addition, pure single-layered graphene is transparent, but graphite is iron black. Fullerene, on other hand, is a closed/partially cage-like structure made up of hexagonal, pentagonal, and heptagonal carbon rings. The additional pentagonal and heptagonal rings allow for the formation of sphere-like structures, which are not present in pure graphene. Fullerene is denoted as C_n where C is the carbon atom and n denotes the number of carbon atoms present in the structure. The most common fullerene is C_{60} (Figure 1). Fullerene was first predicted in 1970 by Eiji Osawa and was first discovered in 1980 by Sumio Iijima. Fullerene is bonded together by single or double covalent bonds with the absence of a pi cloud. The electrical conductivity of fullerene is lower than that of graphene and graphite, which makes it useful for semiconductor applications such as solar cells and diodes. Fullerene is also used in the medical area as an antibacterial agent and gas absorbent. It can also be used for the synthesis of carbon nanotubes [14]. Carbon nanotubes, also called cylindrical fullerenes, have long tubes shaped as one-dimensional structures whose ends are capped by fullerenes. Carbon nanotubes can be considered as a rolled-up graphene sheet that has a diameter in the range of tens of nanometres and lengths of up to a few millimetres. There are two major types of carbon nanotubes: single-walled and double-walled. Carbon nanotubes have the highest measured tensile strength, with good electrical and thermal conductivity. Due to their unique properties, they can be utilized for energy storage devices, thin film electronics, medical applications,

and more. The other major types of derivatives of graphene which are directly obtained by the chemical reactions of graphene include hydrogenated graphene called graphane, fluorinated graphene called fluorographene, and oxidized graphene called graphene oxide. These derivatives of graphene are discussed in detail in the following sections.

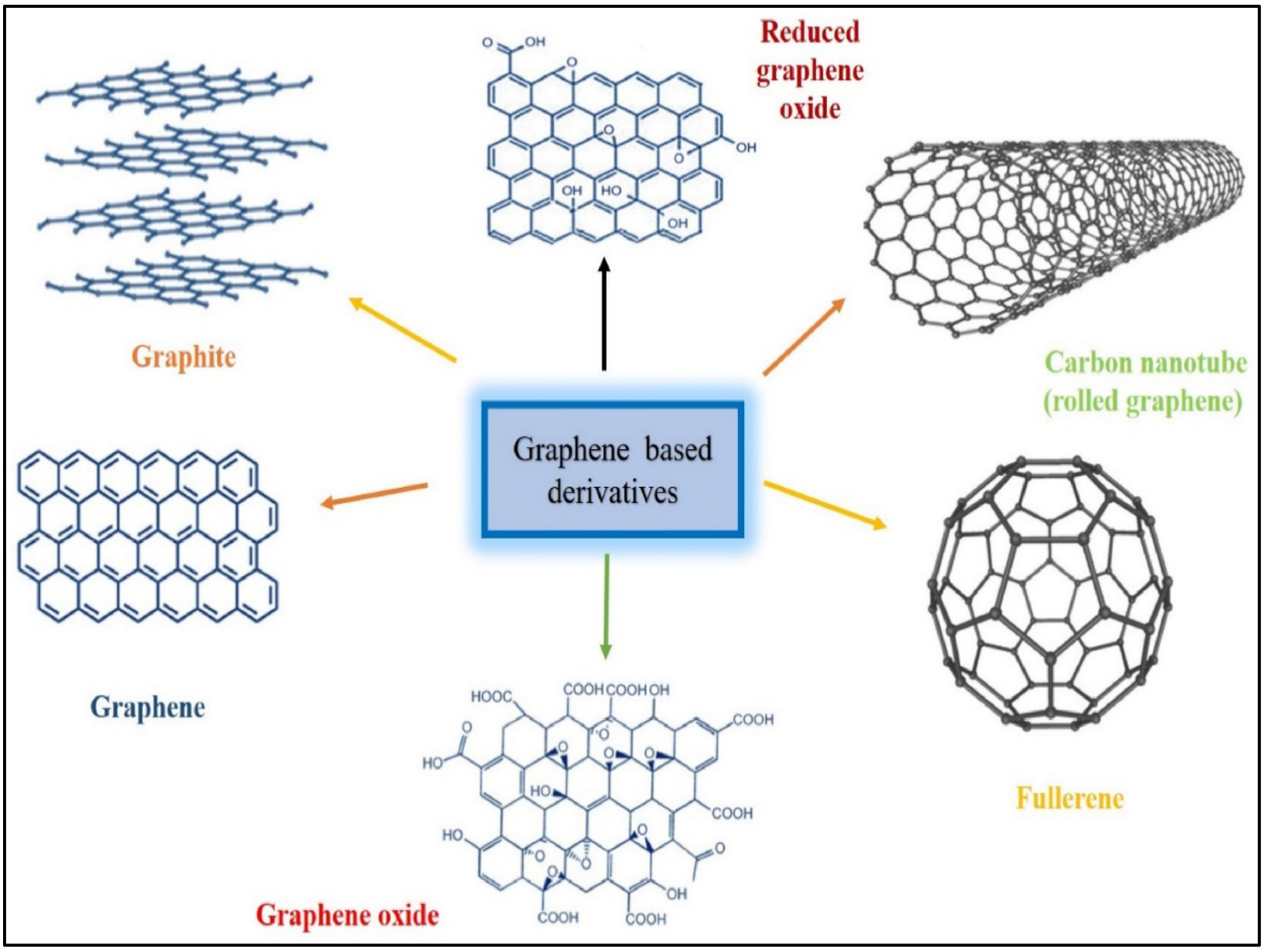

Figure 1. Graphene and its derivatives [15].

1.1.1. Graphane

Hydrogenated graphene, the product of partial hydrogenation, was reported in 2007, for the first time, by Sofo et al. [16]. The C-H bonds in graphane can be formed only if the carbon atoms change their hybridization from sp^2 to sp^3. This makes the graphene layer soften, which makes it possible for the C-H bonds to form. The exact binding of every carbon atom to a hydrogen atom cannot be achieved by a single mechanism. This occurs because the hydrogen atoms may join the graphene layer from either above or below. There are three configurations of graphane that are particularly well known and stable: chair configuration, stirrup configuration, and boat configuration, as provided in Figure 2. Various additional structures have also been postulated, such as the twist-boat, the twist-boat-chair, the armchair, the tricycle, and many more; nevertheless, all these configurations are considerably less stable than the above three graphane configurations, and consequently, they are of limited relevance [17]. Yang et al. studied the optical and electronic properties of graphane using the ad initio pseudopotential density functional method. It was observed that with decreasing graphane width, there is an increase in the band gap. The reason for this was the quantum confinement effect, as it was found that quantum confinement has no impact on the optical properties of graphane. It was also observed that, unlike for graphene, the optical properties of graphane do not depend on their width and edge shapes. These unique optical properties make graphane useful

for various nano-scale optics and optoelectronic devices [18]. Nagarajan et al. used the ab-initio technique to study the adsorption behaviour of NO_2 and SO_2 gases on graphane nanosheets and nanotubes. It was found that the interaction of the toxic gases with the graphane caused a change in their energy band gap. The observed NO_2 and SO_2 adsorption energies are in the range of 0.5 and 0.3 eV, respectively. In addition, the change in the energy gap of the system was found to vary between 34.67 and 55.95% for the graphane sheets with NO_2 adsorbed, with 87.3 and 151.45% for the graphane sheets with SO_2 adsorbed. This resulted in a shorter recovery time for SO_2 desorption. Their study showed that nanosheets and nanotubes of graphane can be used to efficiently detect smaller gas molecules such as NO_2 and SO_2 [19].

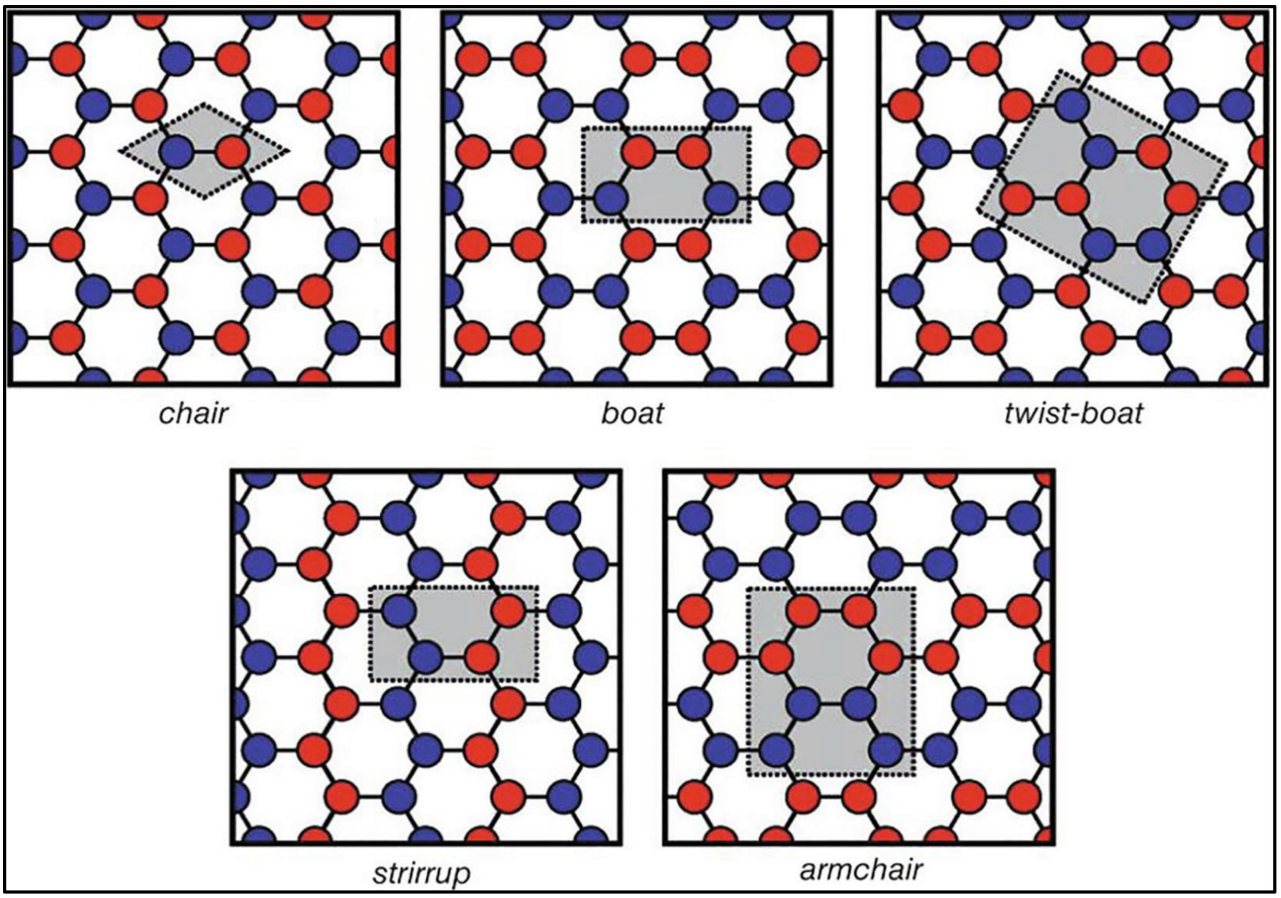

Figure 2. Five different configurations of graphane where the carbon atom is equivalent. Here, the blue- and red-coloured dots represent the adsorption of hydrogen above and below the layer of graphene [17].

1.1.2. Fluorographene

The first fluorinated graphene was identified as fluorographene. It shows different properties than pure graphene. Sometimes, it is also referred to as the thinnest possible insulator because its conductivity is very low in comparison to graphene. Similar to graphane, it has a fluorine atom bounded above or below the carbon layer [20]. Controlling the microstructures of high-quality fluorinated graphene offers a lot of potential in changing the different traits such as layer, size, and surface chemistry. Fluorinated graphene has a wide range of superior properties, including a broad bandgap of 3.1 eV (based on the change from trigonal sp^2 orbital to tetragonal sp^3 orbital), strong thermal stability below 400 °C, and high hydrophobicity, which helps with its use in potential applications such as energy conversion and storage devices, electrochemistry and supercapacitors [21]. Hrubý et al. reported a study on the properties of two commercially available fluorinated graphene types

(highly fluorinated and less fluorinated graphene). X-ray diffraction, Raman, and X-ray photoelectron spectroscopy were used to determine its structural properties. Photoluminescence spectroscopy and diffuse reflectance were used to determine its optical properties. It was observed that the highly fluorinated graphene had well-defined adsorption at 5.75 eV. The ab initio calculations showed that the reason for this observed absorbance was the excitation peak. On the other hand, less fluorinated graphene showed two absorbance peaks at 2.87 and 4.81 eV. Raman mapping showed the presence of inhomogeneity in the samples with the presence of a defluorinated area. Their study showed that structural deformities harmed the properties of fluorinated graphene [22]. Wei et al. prepared fluorographene using low-pressure chemical vapor deposition. There were three layers of monolayer graphene which were grown and transferred to silicon nitride substrate. Raman spectrum and X-ray photoelectron spectroscopy confirmed fluorination of the graphene layers. The pH sensitivity of the prepared samples showed an efficiency of 56.8 mV/pH. This reported study showed excellent pH-sensing performance for potentiometric sensors [23].

1.1.3. Graphene Oxide

The oxygenated form of graphene is known as graphene oxide (GO). Graphene oxide was discovered in the year 1859 by Benjamin Brodie much before pure graphene. He performed a series of chemical reactions by subjecting the graphite to some strong concentrated acids and then discovered a new material, named "graphon". Later, he called it carbonic acid, a new form of carbon-based material. Its importance was not recognized at that time until graphene was discovered in 2004 [24,25]. GO is a kind of two-dimensional material that has a honeycomb-like carbon structure and is paired on both sides with oxygen functional groups. These functional groups contribute in some way to the characteristics of GO, such as magnetic susceptibility, band gap, and conductivity. These properties make GO useful in various applications such as making transparent and flexible conductors, LEDs, field effect transistors, medical sensors, wastewater treatment, and many more [26–31]. GO can be synthesized either by the exfoliation or by the mechanical stirring of graphite oxide [32], and graphite oxide is obtained by using Hummer's approach in which the graphite is oxidized in the presence of strong acids and potassium permanganate. Another useful derivative of graphene is the reduced graphene oxide (rGO), which has a considerably low number of oxygen functional groups present in it. rGO is obtained by reducing graphene oxide by various means such as thermal, electrochemical, or chemical reduction [33]. For example, rGO can be obtained by treating graphene oxide with hydrazine hydrate or by exposing it to strong pulsating light such as hydrogen plasma or xenon flash tube [34–36]. Although GO and rGO might have similarities, the ratio of carbon to oxygen in GO structures is very low compared to rGO structures, which are close to having almost no oxygen. Graphene oxide shows insulating/semiconducting behaviour, but on the other hand, rGO shows excellent electrical conductivity [37–39]. RGO can be used in environmental applications, batteries, supercapacitors, printable electronics, etc. [40–42]. These derivatives of graphene with excellent traits open a new door for researchers to work with graphene. Figure 3 shows the comparative structure of graphene, graphene oxide, and reduced graphene oxide. Ciammaruchi et al. used graphene oxide in electrolytic water splitting. They observed that graphene oxide showed extraordinary chemisorption ability towards hydrogen. The density functional theory model showed evidence of the formation of C-H bonds. It was observed that the chemisorption of hydrogen occurred at sp^2-hybridized atoms. The water-splitting process using a graphene oxide cathode led to the formation of hydrogenated graphene (Graphane) and the chemical storage of hydrogen gas. Thus, their study gave insight into the eco-friendly and low-cost method for hydrogen storage and graphane production [43].

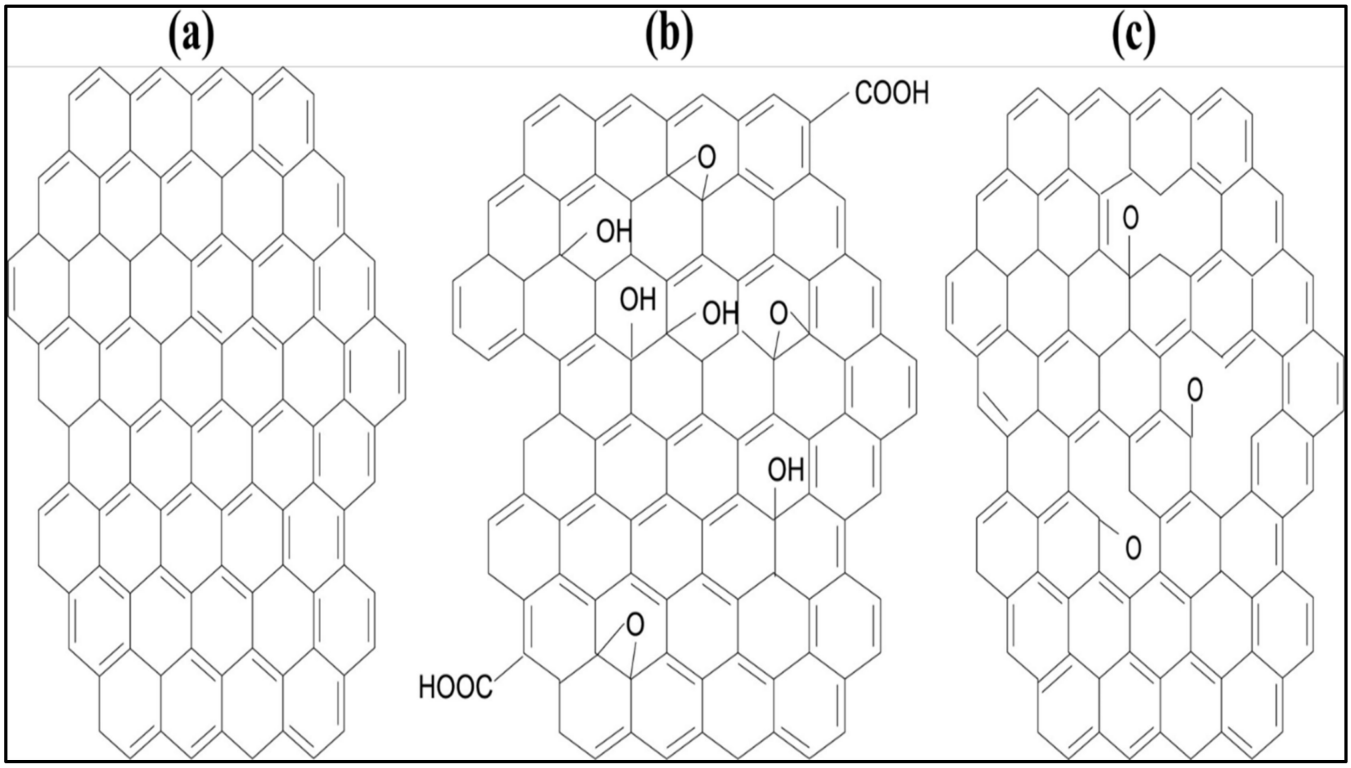

Figure 3. Structure of (**a**) graphene, (**b**) graphene oxide (GO), and (**c**) reduced graphene oxide (rGO) (reprinted with permission from Reference [44]).

Due to their amazing properties, graphene and its derivatives show promising potential in high-frequency devices [45–47], electronics [48–50], biochemical and medical sensors, photodetectors [51–55], and energy storage devices [56–58]. Additionally, they are known for increasing the lifespan of batteries. They also show potential for use in solar cells, supercapacitors, and wastewater treatment (Table 1).

Table 1. Applications of various graphene-based derivatives.

Synthesis	Composite	Application	Reference
In Situ	Ag/GO and r-GO	Biosensing, Catalysis	[59]
Simple physisorption method	Au-GO and Au-rGO	SERS (Surface-enhanced Raman scattering) and Catalytic	[60]
Oxidation/thermal reduction process	Ru/rGO and Rh/rGO	Catalysis	[61]
In Situ	TiO_2/GO	Photocatalysis	[62]
In situ	MnO_2/GO	Supercapacitor	[63]
Electrochemical Deposition	ZnO/rGO	Photovoltaics	[64]
Chemical Vapor Deposition	Graphene/Ni/Cu	Transistor	[65]
Mechanical Exfoliation	Few-layer graphene	Supercapacitors electrodes	[66]

2. Synthesis Methods for the Preparation of Graphene and Its Derivatives

Graphene and its derivatives can be prepared by using top-down and bottom-up approaches. The top-down approach starts with the structural disintegration of a precursor material such as graphite and then continues to the interlayer separation, which finally

results in the synthesis of graphene sheets [67]. For example, arc discharge, oxidation–reduction of GO, liquid phase exfoliation, and mechanical exfoliation are examples of the top-down technique. On the other hand, the bottom-up method employs the use of carbon source gas to create the graphene on a substrate. This method encompasses chemical vapor deposition, epitaxial growth, and complete organic synthesis [1]. The various synthesis methods for the preparation of graphene and its derivatives are discussed below.

2.1. Chemical Vapor Deposition (CVD) Method

The chemical vapor deposition approach is a technique for depositing the gaseous reactants onto a substrate. The substrate acts as a catalyst, and the reaction takes place on the surface of the substrate. Within the reaction chamber, a reaction takes place that results in the formation of a material layer on the surface of the substrate whenever the mixed gases are brought into contact with the substrate. In this approach, at high temperatures (650–1000 °C), hydrocarbon gases such as methane (CH_4), acetylene (C_2H_2), ethylene (C_2H_4), and other biomass materials (solid, liquid, and gaseous carbon sources) are broken down to produce graphene sheets on the metallic catalysts made of copper and nickel. The waste gases are removed from the reaction chamber using a pump, as shown in Figure 4. The substrate is often coated in a very minute quantity at an extremely sluggish pace, and it is measured in microns of thickness per hour. The reaction that occurs in the chamber depends on the nature of the substrate used, for example, if nickel is used as a substrate, the carbon is dissolved on its surface, and the layers of graphene can be obtained by carefully controlling the temperature, i.e., the catalyst is allowed to cool down systematically for controlling the formation of graphene film. On the other hand, if we use copper as a substrate, then the graphene does not dissolve on its surface even at high temperatures. This means that single-layer graphene can be obtained without the need for any complex temperature control if we have copper as a substrate [68]. Therefore, there are various parameters such as type of substrate, gas flow, and temperature which play vital roles in determining the nature of the generated thin film. In addition, many other substrates are used for the production of graphene [65]. For example, Diallo et al., (2021) used germanium with a pit-free surface for the CVD growth of high-quality graphene [69]. Zheji et al., (2021) used a substrate made of microcrystalline diamond for the production of graphene. The produced graphene shows excellent load capacity and durability [70]. Jin et al., (2021) used a platinum substrate to grow graphene in the presence of hydrogen, reported using scanning tunnelling microscope (STN) and low-energy electron microscopy (LEEM) studies. The reported studies show that the prepared graphene is of very high quality with fewer defects [71]. The CVD method can create graphene of high quality with a small number of flaws, a highly linked structure, and a large amount of surface area. However, it has several drawbacks, including high cost of manufacturing, limited productivity, the need for further purification to remove any leftover catalyst, and the transfer of graphene to other substrates. Thus, this method is still far from being commercialized.

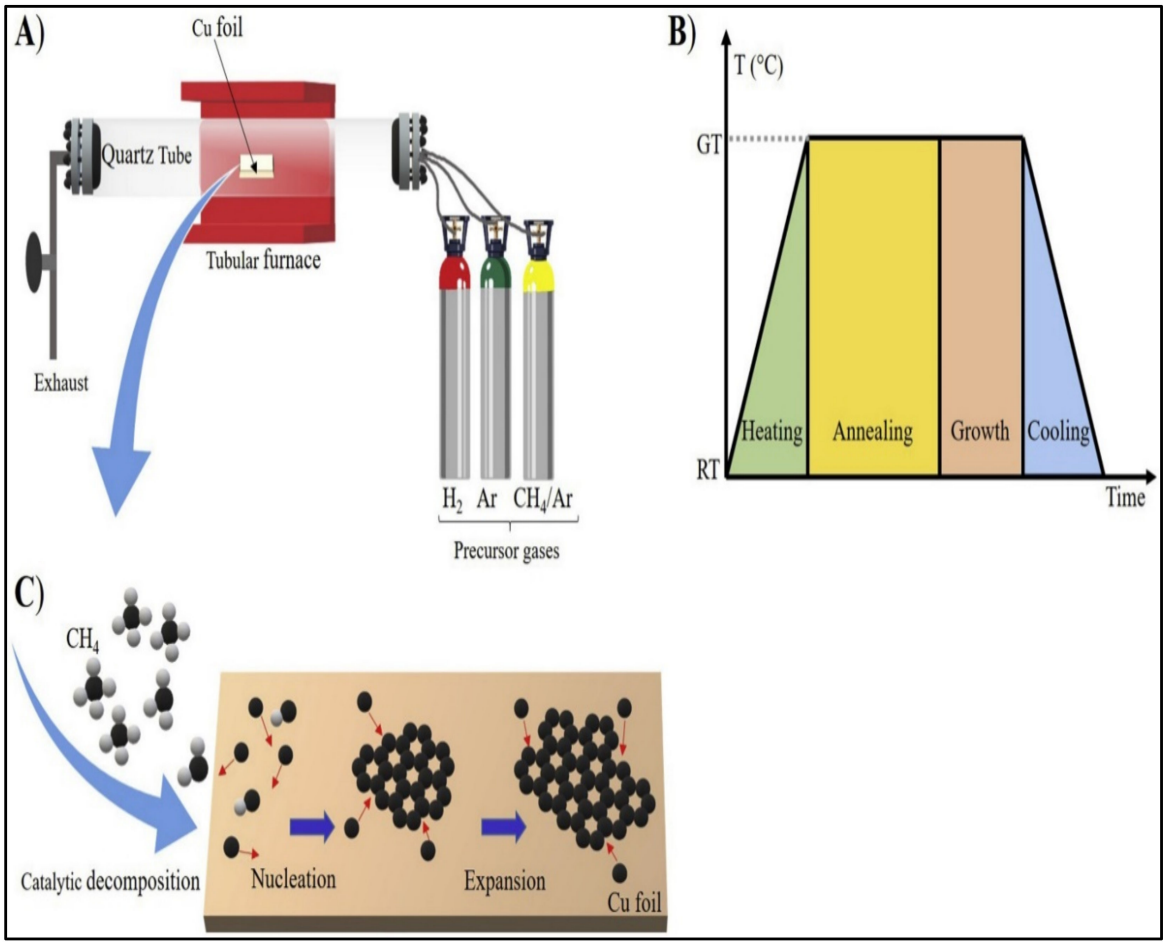

Figure 4. (**A**) Schematic diagram of CVD setup. (**B**) Schematic illustration of standard CVD growth process. RT and GT are room temperature and growth temperature, respectively. (**C**) Growth kinetics of CVD-grown graphene on Cu foil (CH_4 case) (reprinted with permission from [72]).

2.2. Mechanical Exfoliation Method

In 2008, for the first time, the mechanical exfoliation technique was taken into practice for the large-scale production of graphene. It is a top-down technique used for the exfoliation of graphite to form graphene, which involves mechanical energy. Exfoliation simply means peeling up the layers from a surface [73]. In the mechanical exfoliation method, the van der Waal forces must be overcome. Thus, overcoming the attraction forces for removing the layers of graphite to produce graphene is called mechanical exfoliation. It can be conducted in two ways, either by applying normal force or shear force. Recently, peeling graphite with ultra-sharp single-crystal diamond wedges is the synthesis method used for normal force mechanical exfoliation. Mechanical exfoliation can also be performed by other methods such as dry/wet ball milling, sonication, and fluid dynamics methods such as vortex fluid film and mixer-driven fluid dynamics, etc. [73]. Baqiya et al., (2020) created graphene using a coconut shell through an acid-assisted mechanical exfoliation approach. The calculated particle size using TEM investigation was from 1.42 to 4.9 nm [74]. Jayasena and Melkote, in 2015, reported the production of a large area of graphene sheet using the viscoelastic polymer stamp-based mechanical exfoliation technique, and it was about 12 mm $\times$ 12 mm^2 [75]. Hayes et al., (2014) prepared the graphene platelets with mechanical exfoliation in the presence of 1-butyl-3-methylimidazolium hexafluorophosphate, and it was investigated with the help of X-ray photoelectron and Raman spectroscopy. They found that as the grinding time increases, there is a decrease in the size of graphene while the structural deformity increases [76].

2.3. Chemical Exfoliation Method

In this method, graphite is chemically exfoliated when it is exposed to oxidants. This occurs because the oxygen atoms are strong enough to overcome the van der Waal interactions between the graphene flakes. In addition, these oxidants are mixed with strong acids for the manufacturing of GO. Exfoliation of graphene from graphite using alkali metals is another method, which is then followed by dispersion in a liquid medium. Because of the disparity in the ionization potential between graphite and alkali metals, the latter may be used as a template for the formation of graphite intercalation compounds. For instance, the ionization potential of caesium or potassium is lower than that of the electron affinity of graphite (4.34 eV), which substantially increases the intercalation of graphite under low temperature and ambient pressure conditions. The atomic radius of alkali metals is smaller than that of the interlayer spacing of graphite, making exfoliation of the material much simpler [77,78]. This can be an advantage. Chemical exfoliation is a beneficial technique because it can create a big quantity of exfoliated graphene at a low temperature. This ability to produce exfoliated graphene at a low temperature sets the process apart from the other procedures that have been described for the synthesis of graphene. It may also be scaled up and developed to manufacture a variety of functionalized graphene types in a solution process. As a result, it has a bigger relevance in terms of its contribution to technology [79].

2.4. Electrochemical Exfoliation Method

In this method, single-layered or few-layered graphene is obtained by the electrolysis technique. This method requires a graphite electrode, a counter-electrode made up of either platinum or graphite, an electrolyte, and a power supply. When the electric current is passed through the electrodes contained in an appropriate electrolyte, the process of electrolysis occurs and a single-layered or few-layered graphene on the graphite electrode is produced. Most of the time, pyrolytic graphite that is highly oriented is used to make graphite electrodes. In addition, to make the electrode more conductive, sometimes conductive materials (such as tungsten, and carbon stripes) are adhered to the electrodes. To initiate the reaction, a voltage difference is provided to both electrodes; this voltage may be modified to suit individual needs. An example of the electrochemical exfoliation method is shown in Figure 5. Many different ways have been researched to carry out the electrolytic reaction to increase the efficiency of this method [80]. For example, Das et al., (2022) performed electrochemical exfoliation in the presence of a non-conventional electrolyte. They used a polyvinyl alcohol-based gel electrolyte, which led to the development of ultrathin graphene with fewer impurities [81]. Loudiki et al., (2022) used the pencil graphite electrode to produce the GO and rGO materials. The reported results indicate that there is an increase in the electrochemical performance of both these materials [82]. Alshamkhani et al., (2022) prepared the graphene using switching voltage electrochemical exfoliation, and in their research, they found that the efficiency of produced graphene is greater when the switching voltage is applied through the electrode. In addition, the produced samples present better conductivity, with the application of switching voltage [83]. Pingale et al. synthesized graphene by using ultrasonic-assisted electrochemical exfoliation of graphite. In a 500 mL borosilicate beaker, electrochemical exfoliation with ultrasonic assistance was performed. The cathode was made up of a titanium electrode with a Pt coating, while the anode was a pure graphite electrode. With a 5 cm gap between them, the cathode and anode are submerged vertically in the electrolyte. A solution of 4.9 g of H_2SO_4 mixed with 300 mL of distilled water was used to make the electrolyte. This whole arrangement was kept in an external ultrasonic bath as shown in Figure 5a.

The acidic bath helped in the process of exfoliation, by creating bubbles of H_2O and $SO_4{}^{-2}$ between the layers of graphite [84]. Electrochemical exfoliation can be considered one of the most efficient ways to produce graphene and its derivatives. It shows a high yield with a direct approach, but the toxicity of the electrolyte used can become a concern if we use this method on a large scale.

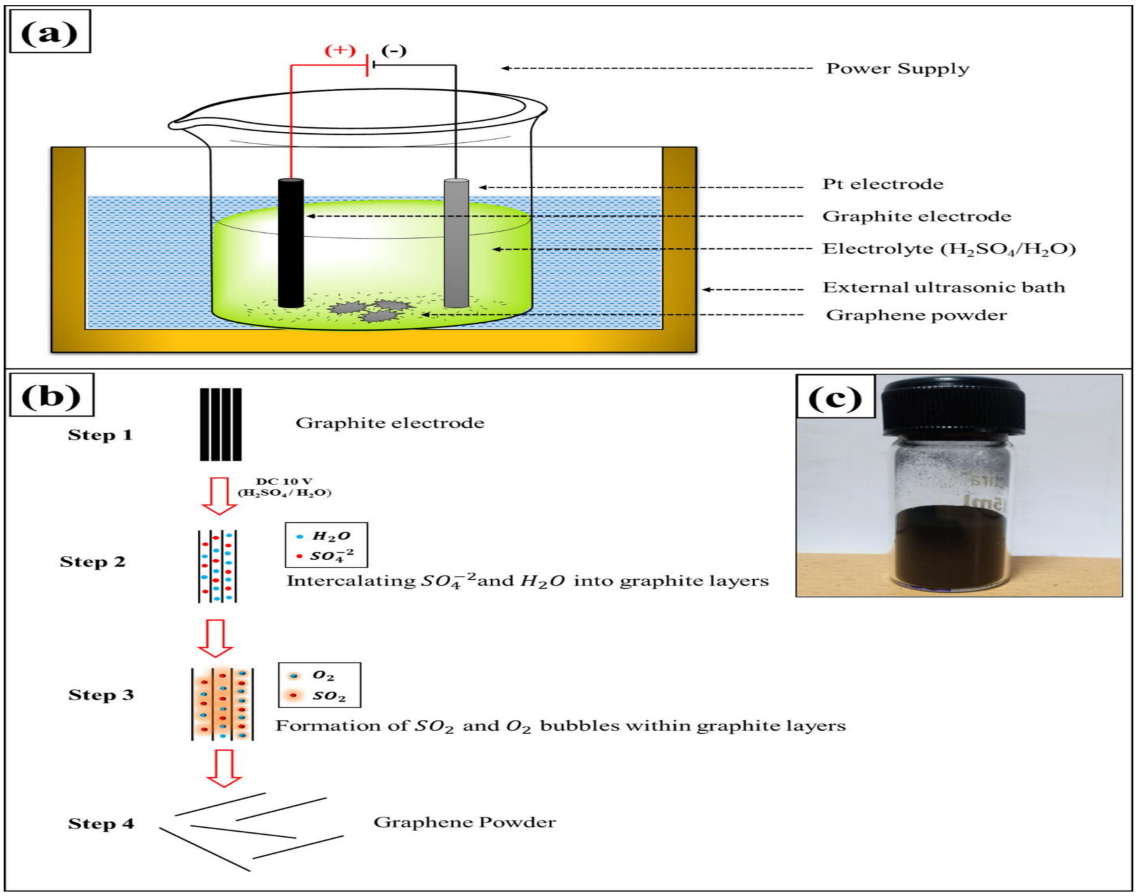

Figure 5. (**a**) Schematic illustration of the ultrasonic-assisted electrochemical exfoliation of graphite. (**b**) The steps in the electrochemical exfoliation mechanism of graphite. (**c**) Picture of exfoliated graphene powder (reprinted with permission from [84]).

2.5. Epitaxial Growth Method

Graphene and its derivatives may be produced by the thermal decomposition of a hexagonal substrate (silicon carbide, SiC) at temperatures ranging from 1200 to 1600 degrees Celsius in the presence of a vacuum or inert gas. Silicon (Si), which has a melting point of 1100 °C, will sublimate when subjected to a high-temperature treatment. This will leave the excess carbon atoms to combine and create an sp^2-hybridized network. This helps in the formation of graphene on a SiC substrate. This process is called the epitaxial growth approach [85]. However, there is a lack of uniformity in the graphene that is created using this process. Many researchers and scientists have used this method to prepare high purity graphene with desirable properties; for example, Liu et al., (2020) prepared graphene with high conductivity using the epitaxial growth approach on 4H-SiC (0001) substrate with a high-power continuous laser [86]. Deng et al., (2020) prepared a single-crystal graphene wafer on the $Cu_{90}Ni_{10}$ substrate using the ultrafast epitaxial growth approach, and they found that the presence of nickel helps in increasing the rate of reaction during the formation of graphene [87]. However, environmental concern is being raised owing to the release of tetrafluoroethylene (C_2F_4) during the synthesis process, despite the production of high-quality graphene. The epitaxial growth of graphene would be too expensive because the process uses a lot of energy and commercial SiC substrates with limited sizes. In addition, the process could lead to the formation of different polar faces, such as the Si-face or the C-face, which lowers the quality of the graphene output. Si-face graphene production is preferred because it makes sure that the graphene is made steadily and consistently. This method makes it easy to change the number of graphene layers, which depend on the temperature at which they are heated. This synthesis approach is still being evaluated

since there is a lack of information on the growth processes and interactions between the graphene and the substrate [88]. The various advantages and disadvantages of all synthesis methods for the fabrication of graphene and its derivatives were listed in Table 2.

Table 2. Advantages and disadvantages of different synthesis methods of graphene and its derivatives.

Synthesis Methods	Advantages	Disadvantages	References
Chemical vapor deposition	High-quality graphene with high yield	High cost	[89]
Mechanical exfoliation	Cost-efficient and high-quality graphene production	Low Yield	[73]
Chemical exfoliation	Rapid process and high-quality graphene production with high yield	Uses toxic chemical and have toxic by-products	[79]
Electrochemical exfoliation	High yield (commercialized)	Can contain impurities between graphene layers	[90]
Epitaxial Growth	High-purity graphene production	Time-consuming with low Yield	[85]

3. Properties of Graphene and Its Derivatives

The various properties of graphene and its derivatives will be covered in this section. The graphene-based derivatives, graphane, fluorographene, and graphene oxide, exhibit several interesting properties, including those relating to structural, mechanical, and optical characteristics.

3.1. Structural Traits

In this section, we reported the structural parameters of graphene and its derivatives (Table 3). Some of these parameters are bond length (d_{CX}, d_{CC}, C = carbon, X = hydrogen, fluorine), bond angle (θ_{CCX}, θ_{CCC}, C = carbon, X = hydrogen, fluorine), and lattice constant (a).

Table 3. Structural properties of graphene and its derivatives.

	d_{CX} (Å)	d_{CC} (Å)	Θ_{CCX} (Degree)	Θ_{CCC} (Degree)	a (Å)	References
Graphene	-	1.42	-	120	-	[91]
	-	1.421	-	120	2.46	[92]
	-	1.425	-	120	2.468	[93]
	-	1.42	-	120	2.46	[94]
	-	1.42	-	120	2.46	[95]
Graphane	1.111	1.533	107.45	111.39	2.532	[93]
	1.11	1.53	107.43	111.42	2.54	[92]
	1.12	1.52	107.35	111.51	2.51	[94]
	1.111	1.53	-	-	2.54	[96]
Fluorinated graphene	1.37	1.55	108	111	2.55	[97]
	1.383	1.581	-	-	2.606	[98]
	1.38	1.58	-	-	2.61	[99]
	1.371	1.579	-	-	2.6	[91]
Graphene oxide	1.095	1.41	-	120.1	-	[100]
	1.094	1.41	-	120.1	-	[100]
	1.095	1.41	-	120.2	-	[100]

3.2. Mechanical Traits

3.2.1. Graphene

The thing that makes graphene stand out as a reinforcing agent in composites is that it has very interesting mechanical properties. Graphene's outstanding mechanical qualities are due to the stability of the sp^2 bonds that make up its hexagonal lattice and that fight against a wide range of in-plane deformations. These bonds are responsible for the material's exceptional strength [101]. Graphene is not just the material with the highest measured strength but also the one with the maximum stiffness [17]. The elastic modulus (E), Poisson's ratio, and intrinsic strength of graphene are its most fundamental phenomenological mechanical properties [102]. Frank et al., (2007) [103] calculated an elastic modulus of 0.5 TPa (terapascal) for a stack of graphene sheets ($n > 5$), while Lee et al., (2008) [104] reported an elastic modulus of 1.02 TPa for a graphene monolayer. Zhang and Pan (2012) [105] evaluated the elastic modulus of monolayer (0.89 TPa), bilayer (0.39 TPa), and multiple-layer graphene sheets using an instrumented nano-indenter. They found that the elastic stiffness of graphene decreases with the number of layers. The strain caused by a pressure differential between the graphene membranes was measured by Lee et al., (2008) [104] using Raman spectroscopy, and therefore, a substantially higher elastic modulus was determined. The estimated elastic modulus of monolayer and bilayer graphene are 2.4 and 2.0 TPa, respectively. Poisson's ratio values are often calculated through the numerical simulations because they cannot be tested in experiments in a direct way. The inverse analysis of the free-standing indentation data by Lee et al. yields an estimate of intrinsic strength of 130 GPa (gigapascal) for the graphene monolayer (the thickness of graphene is assumed as 0.335 nm).

3.2.2. Graphane

The computational method is one of the methods that Qing Peng and his colleagues used to investigate the mechanical characteristics of graphane. Graphane is shown to have a non-linear elastic deformation up to an ultimate strain, which is 0.17, 0.25, and 0.23 for the armchair direction, zigzag direction, and biaxial direction, respectively. An anisotropic characteristic may be seen during deformation and failure as well as in ultimate strength. The ultimate strength of the material under biaxial strain is 0.07 N m^{-1} higher than the ultimate strength of the material under armchair strain, but it is 0.01 N m^{-1} lower than the ultimate strength of the material under zigzag strain [106]. The Poisson ratio of graphane is the lowest of all the monolayer honeycomb structures that are currently known. Due to its superior mechanical qualities, it is a promising contender for use in the construction of tubes or pipelines that are capable of transferring materials at faster speeds while subjected to high pressure. With the increase in pressure, there is a consistent and gradual drop in Poisson's ratio [106]. The 2D Young's modulus (E′) and Poisson's ratio were determined to be 243 Nm^{-1} and 0.10 for the chair-type hydrogenated graphene isomers while for the boat-type hydrogenated graphene isomers, they were determined as 230 Nm^{-1} and −0.01 [100].

3.2.3. Fluorinated Graphene

The process of fluorination will often affect the mechanical properties of graphene, due to the existence of carbon–fluorine (C-F) bonds. These properties include Young's modulus (E′) and intrinsic strength (σ). Fluorographene displayed both a lower "E′" of 100 Nm^{-1} and a lower "σ" of 15 Nm^{-1} than the other compounds as reported by Feng et al., (2016) [107]. The Young's modulus and Poisson ratio of fluorographene in two dimensions were 226 Nm^{-1} and 0.10 as shown by Leenaerts et al., (2010) [100].

3.2.4. Graphene Oxide

First-principle simulations are being used to learn more about the mechanical properties of graphene oxide, such as its Young's modulus and intrinsic strength. The structural models of both ordered and amorphous graphene oxide have been compared and con-

trasted. As the percentage of oxygen groups in an ordered graphene oxide varies, Young's modulus is observed to shift between 380 and 470 (GPa). The difference in the Young's modulus of amorphous graphene oxide with equivalent coverage is less and ranges from 290 to 430 GPa. In a similar view, ordered graphene oxide has been shown to exhibit better inherent strength when compared to its amorphous counterparts. Due to the splitting of the sp^2 carbon network and reduction of the energy stability for the ordered and amorphous graphene oxide, Young's modulus and the intrinsic strength show a decline in a monotonic fashion [108]. To reduce the amount of oxygen that was present in the production of graphene sheets, GO was electrophoretically deposited using the electrophoretic deposition (EPD) process. In addition to this, the polydimethylsiloxane (PDMS) substrate was used in the direct production of large-scale GO films using transfer procedures. Films with thicknesses ranging from 100 to 200 nm have Young's moduli of 324 to 529 GPa [109].

3.3. Optical Traits

3.3.1. Graphene

Graphene has a two-dimensional structure, which greatly affects its optical properties as well as band gap. Because there is less screening in two-dimensional materials, the electrons and holes interact with each other, causing the location of the bound exciton states to be at a significant distance below the conduction band [110]. Robinson and his colleagues found that the graphene material becomes clear in the visible spectrum after being treated with XeF_2 gas. The graphene displays an absorption edge at 2.5 eV, which was in excellent accordance with the prominent van Hove singularity [111]. Graphene's energy band structure was no longer linear above 2.5 eV. Jeon et al. [112] found that the PL spectra of graphene dispersed in acetone could be obtained at ambient temperature by utilizing an excitation wavelength of 290 nm (4.275 eV). The findings demonstrated that a graphene sample with an empty bandgap did not produce any emission.

3.3.2. Fluorinated Graphene

Fluorine atoms may be substituted in place of carbon atoms on graphene, which results in substantial changes to the material's optical traits, such as absorption band, photoluminescence, and transparency. Fluorinated graphene exhibited low-intensity absorption compared to graphene. This absorption was characterized by a weak and wide band that ranges from 4.0 to 5.0 eV. Because of the dispersion caused by impurities, it had a high degree of transparency over the whole spectrum. In addition, fluorographene could only take in light with an energy greater than 3.0 eV. Based on these findings, fluorographene seemed to be transparent in the region of visible light with a broad bandgap of 3.0 eV in a practical way [113]. According to research performed by Zhao and his colleagues, the fluorinated GO dispersed in acetonitrile (CH_3CN) exhibited two absorption peaks at approximately 220 and from 250 to 350 nm. These peaks were attributed to the π–π * transition of conjugated polyene-type structures in the carbon nanosheets and a couple of conjugated aromatic domains with different sizes [114]. Jeon et al., (2011) recorded the PL spectra of fluorinated graphene at room temperature by using the excitation wavelength of 290 nm. According to the findings, fluorinated graphene has two emission peaks, one at 3.80 eV and the other at 3.65 eV, suggesting large bandgaps [112].

3.3.3. Graphane

Similar to graphene, graphane has a two-dimensional structure which causes a substantial influence on its optical traits and therefore greatly lowers the optical band gap. With the HSE06 functional, the reported values of the DFT band gap were much bigger than those from the PBE calculations, but they were much smaller than those from all the GW calculations. On the other hand, all GW-type calculations gave the same band gaps, even though the band structures were different. At the highest GW-HSE06 level, the band gap of chlorographene was predicted to be smaller than those of fluorographene (8.3 eV) or graphane (6.2 eV). Using the Bethe–Salpeter equation, it was found that the optical

absorptions of chlorographene happen at much lower energies. This is because the binding energies of excitons are high for chlorographene, fluorographene, and graphane (1.3, 1.9, and 1.5 eV), respectively. The band gaps and absorption energies were both lowered by point defects [115].

3.3.4. Graphene Oxide

Rattana et al., (2012) reported the synthesis of graphene oxide nanosheets by the exfoliation of graphite oxide powder. The various characterization techniques such as Raman spectroscopy, FTIR spectroscopy, UV–Vis spectroscopy, and photoluminescence spectroscopy were used to investigate the optical characteristics of the as-prepared GO nanosheets. The findings of the FTIR analysis indicated that the oxygen-containing groups were present in the GO nanosheets, and a wide emission band at 450 nm in the visible range was confirmed by the PL study [116]. Goumri et al., (2016) reported the synthesis of nanocomposites made from polyvinyl alcohol (PVA) with low graphene oxide (GO) and partially reduced graphene oxide (PRGO) loadings using the aqueous solution in both the acidic (pH ~4) and neutral medium (pH ~7). The synthesis was carried out to report the optical properties of the GO/PRGO-based nanosheets. The PL spectra of GO and PRGO with PVA nanocomposite films were measured between 400 and 900 nm. A wide blue-green emission from PVA was seen at 497 nm, and two peaks were seen at 619 and 683 nm. This is caused by the n-π^* electrons' $2p^2$ (O) movement in O-H functional groups. The phenomenon of fluorescence from the GO was observed at 464, 628, and 703 nm. In addition, the photoluminescence of GO is caused by the electron-hole recombination from the bottom of the conduction band (CB) and areas close to it [117].

4. Graphene and Its Derivative-Based Composites

Graphene and its derivatives can form a variety of composites. For example, graphene composites with metal–organic frameworks show an increase in overall stability. In addition, composites of graphene with hydrogel show an increase in adsorption ability, and composites of graphene with semiconductor show better results in photocatalysis and electrical properties. These composites give promising results in various applications such as photocatalysis, wastewater treatment, batteries, supercapacitors, etc. Some of these composites are discussed in this section.

4.1. Graphene with Metal–Organic Frameworks

Metal–organic frameworks (MOFs) are a kind of organic–inorganic hybrid crystalline material with high porosity that consists of a regular array of positively charged metal ions surrounded by organic molecules [118]. These organic molecules are also known as linkers. The metal ions form nodes that connect the arms of the linkers, which create a structure that is similar to a cage and has a repeating pattern. Because of their hollow nature, they have an exceptionally high interior surface area. Utilizing the cage-like structure of MOFs, several applications are being developed for use in a wide variety of industries. Some examples of these applications include gas storage and separation, liquid separation and purification, electrochemical energy storage, catalysis, and sensing. In addition to their use in direct applications, metal–organic frameworks (MOFs) have been put to use as one-of-a-kind precursors in the production of inorganic functional materials [119]. These include carbons, metal-based compounds, and their composites. However, they have many advantages and come with their share of flaws. The main drawback of MOFs is their low stability. To counter this flaw, many researchers have tried to make composites of MOFs with different materials. Out of many composites, graphene has come out as an excellent material to counter the stability problem of MOFs [120]. In addition, graphene and MOFs composites can be used in many applications. Some of the research performed on these composites is discussed here. Li et al. prepared a core–shell structure 3D-graphene/Fe_3O_4@N-C composite for microwave applications in their investigation. They discovered that adding graphene made composites lighter and changed the composites' electromagnetic parameters [121]. Liu et al. made

MOF-derived carbon/N-doped three-dimensional reduced graphene oxide composites that obtained excellent electrochemical performance and high specific capacitance because of the introduction of graphene for capacitive deionization [122]. Li in 2022 prepared MOFs and graphene oxide composites for photocatalytic degradation application and found that the composite UiO-66 (Ce)/GO showed almost three-fold improvement in performance than the pure UiO-66 (Ce) [123]. Bai et al. prepared FeMn-MOF and FeMn-MOF/G composites and found that the composites showed excellent microwave absorption ability compared with their pure form, as shown in Figure 6 [124]. Tang et al. prepared graphene and MOFs co-modified composites and found that the introduction of RGO and MOFs shows enhanced photocatalytic ability under ultraviolet and visible regions, and an increase in adsorption capacity was observed [125].

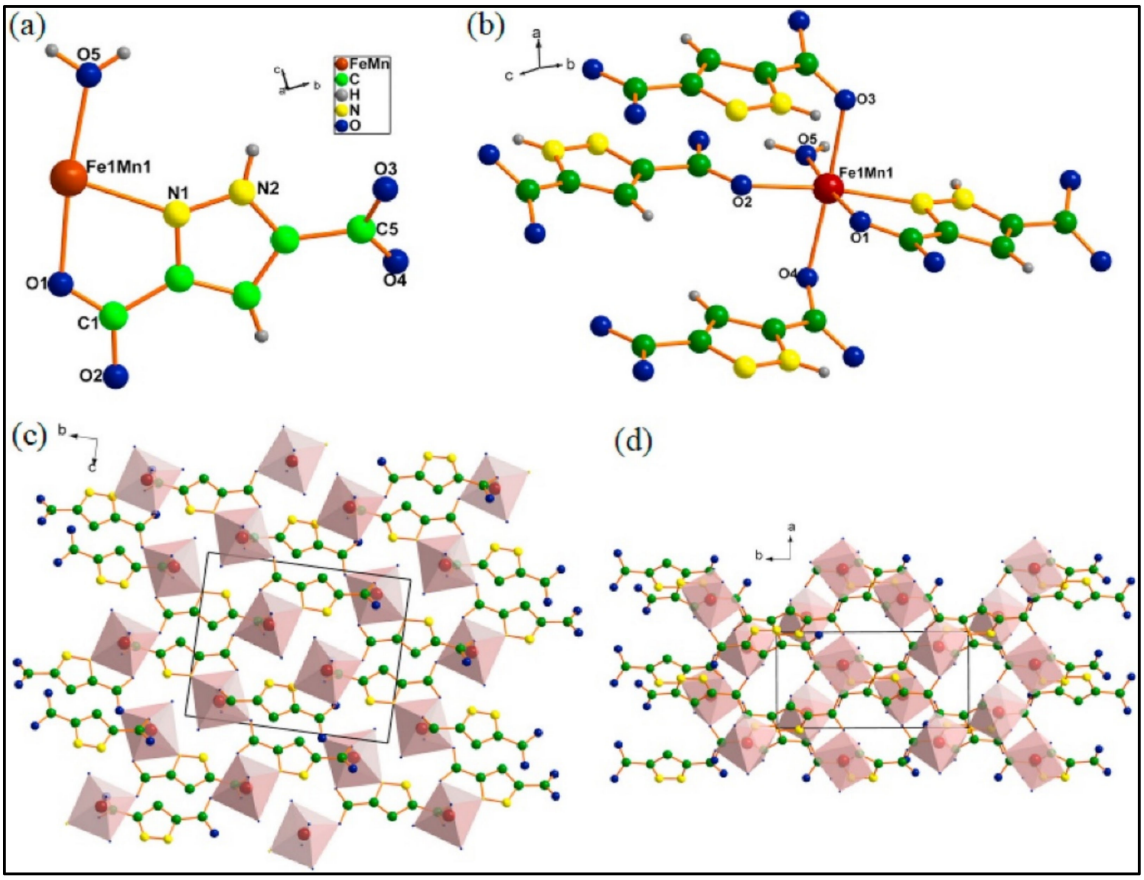

Figure 6. Scheme of crystal structure of 35pFeMn: (**a**) asymmetric unit, (**b**) FeMn coordination system, (**c**) unit cell along *a* direction, and (**d**) unit cell along *c* direction (reprinted with permission from [124]).

4.2. Graphene Composites with Semiconductors

Semiconductors are being used in various modern applications. They are used in various technologies from light bulbs to hydrogen production. They show great potential because their properties can be enhanced drastically when formed as composites with other materials. Graphene composites with semiconductors have shown enhanced performance in various applications such as wastewater treatment, hydrogen production, energy production, water splitting, etc. [126–128]. Lu et al. reported an increase in photocatalytic activity for graphene–semiconductor composites [129]. Serry et al. reported a novel multi-model system for energy conversion using graphene/metal/semiconductor composites [130]. Chen et al. prepared a $BiVO_4$/MIL-53(Fe)/GO photocatalyst which showed excellent photocatalysis compared with $BiVO_4$. In addition, they found a reduced recombination rate of electron and hole pairs generated during the process [131]. Dash et al. prepared a graphene/silicon composite which showed an increase in electrical conductivity compared

with pure Si [132]. Mallik et al. prepared RGO/SnO_2 which showed strong PL emission and strong capacity in optical applications, as provided in Figure 7 [133].

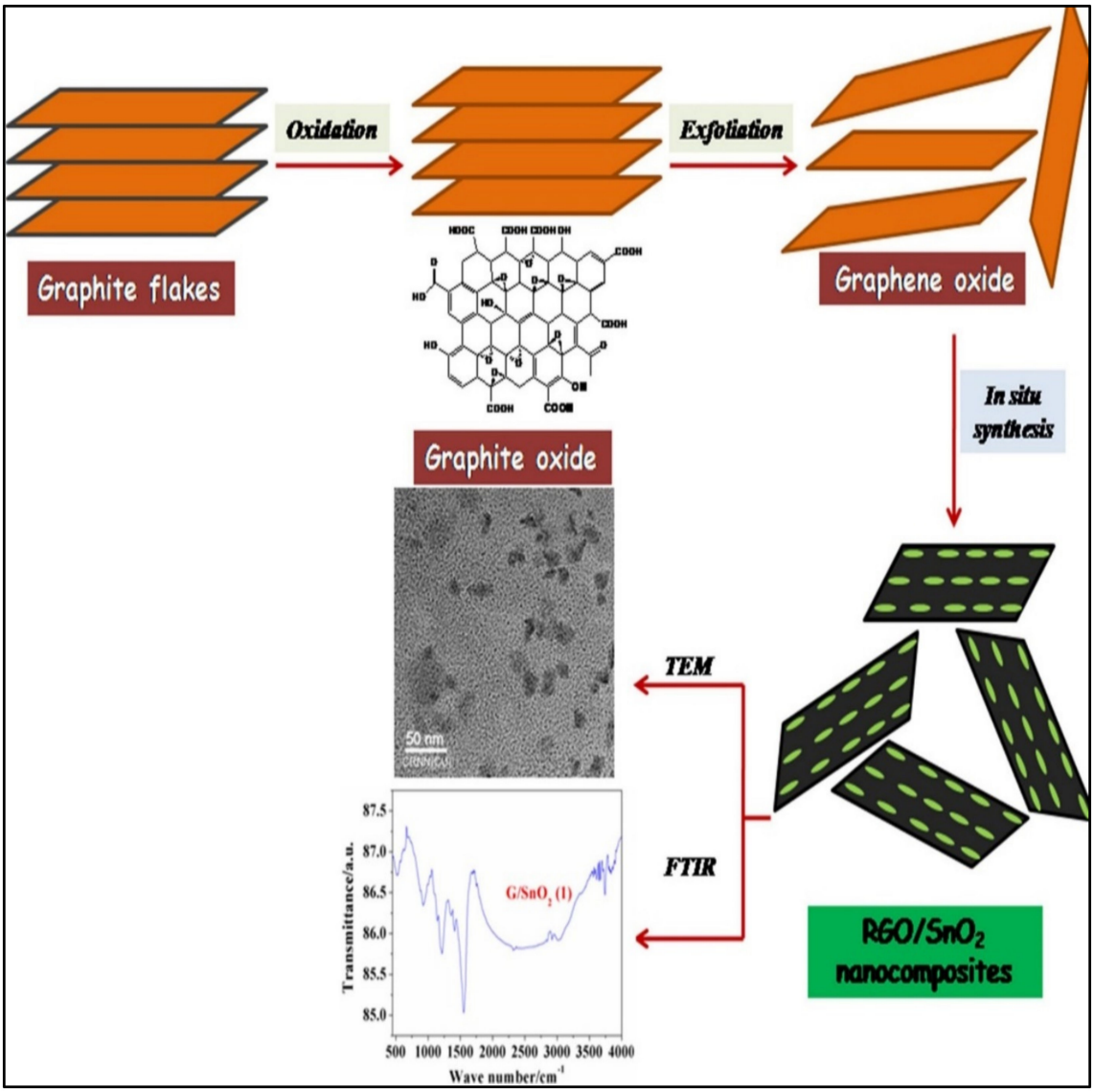

Figure 7. In−situ schematic representation of graphene-based SnO_2 nanocomposite (reprinted with permission from reference [133]).

4.3. Graphene Composites with Polymer

A polymer, as the name suggests, is made up of multiples of monomers. Their properties such as resilience, resistance to electrical and thermal conductivity, refractive index, permeability, and even crystallinity make them very useful for a variety of applications. Polymer composites with graphene have shown their importance in various modern-day technologies. For example, Saran et al. prepared a graphene oxide/polymeric porphyrin composite. Their results showed that the presence of graphene oxide increased the reduction of dioxygen in oxygen reduction reactions [134]. Hamidinejad et al. made a graphene/polymer nanoplatelet composite foam in 2022. They obtained significant variation in electrical properties such as permittivity and thermal and electrical conductivity. In addition, the EMI shielding effect showed an increase of almost 45% [135]. Yao et al. made a micro-supercapacitor based on an open shell polymer/graphene composite with excellent feats such as high power and energy density; it also showed excellent stability [136]. Oni and Sanni prepared polymer/graphene/MOF (MIL-53(Cr)) for the degradation of

dichlorophenol. The prepared sample showed an increase in adsorption ability and easy removal of adsorbent from water [137]. Gong et al. introduced graphene layers in a carbon fibre/polymer composite and found improvement in the damping properties of the material [138].

4.4. Graphene Composites with Hydrogel

Hydrogels are cross-linked 3D polymers that absorb and hold water. Due to their customizable qualities and versatility, hydrogels are employed in tissue engineering, regenerative medicine, wastewater treatment, and soft robotics. Many researchers have been drawn towards hydrogel and graphene composites because of their various uses in energy, environmental, and biomedical applications. For example, Zhang et al. were able to obtain excellent gravimetric and volumetric capacitances using nanocellulose/N, O co-doped graphene composite hydrogels [139]. Noureen et al. prepared a $BiVO_4$/RGO composite hydrogel for decontaminating polluted water. The prepared sample showed enhanced photothermic and photocatalytic performances [140]. Wang et al. prepared RGO/$Cu_{7.2}S_4$ hydrogel with an improvement in solar thermal conversion efficiency by around 96% under one sun illumination (Figure 8) [141]. Fong et al. made a reduced graphene oxide hydrogel composite for the demulsification of crude oil in water, obtaining 82.16% efficiency and showing excellent reusability results up to six times with a small reduction in degradation rate each time [142]. Meng et al. prepared a siloxene/RGO composite hydrogel for supercapacitors and found that graphene introduction increased capacitance performance and cycling stability [143].

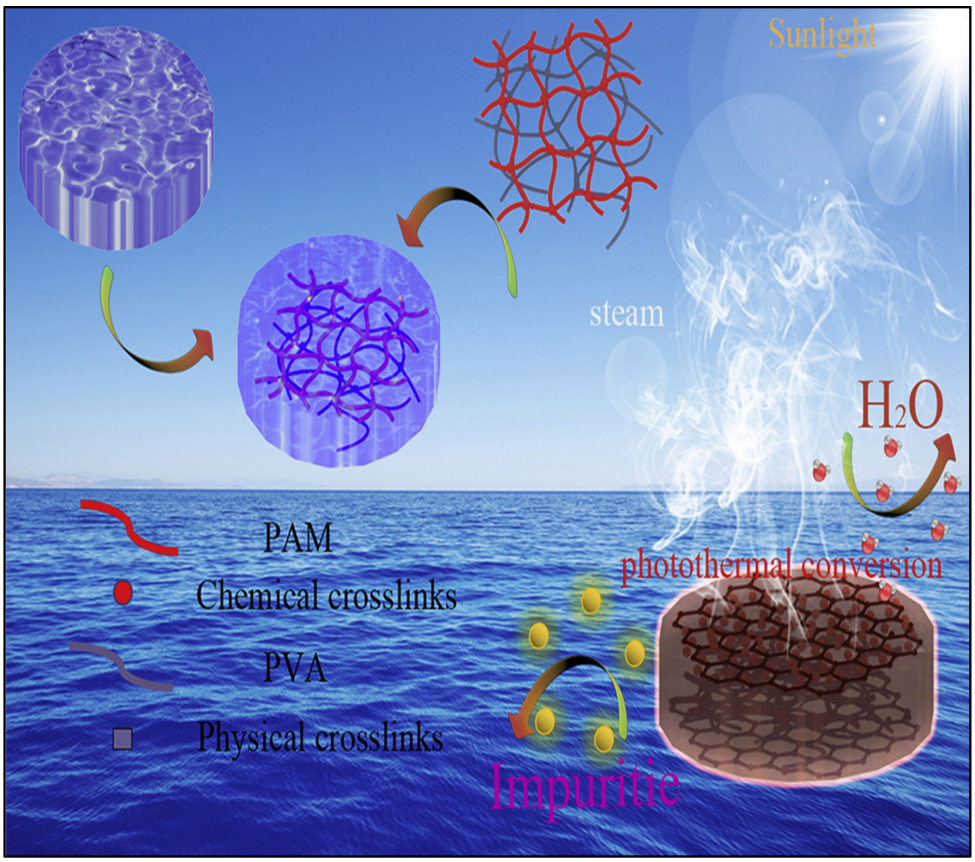

Figure 8. Schematic representation of mixed hydrogel device produced by solar steam generation (reprinted with permission from reference [141]).

5. Environmental Applications of Graphene and Its Derivative-Based Composites

The environment has been harmed by human activities in many ways, which has resulted in poor human health, an increase in diseases, and the deaths of not only humans

but also other species of life. Human activity has caused many types of pollutants to enter our ecosystem. Some of these pollutants include heavy metals, dyes, poisonous gases, harmful chemicals, pesticides, crude oil, and many other things [144]. To counter this, many researchers are still researching how to efficiently detoxify our environment that is full of these harmful elements [145]. Some of the methods used to remove these pollutants are adsorption, absorption, chemical reduction, physical removal of pollutants, biological treatment, photocatalytic degradation, etc.

Graphene and its derivatives can become powerful materials for environmental detoxification, specifically wastewater treatment. Their magnificent properties can enhance the work of many conventional methods for environmental detoxification. The three main ways which can utilize the properties of graphene for environmental applications are adsorption, photocatalytic degradation, and filtration. There are other ways by which graphene can be used to separate pollutants from the water or air, such as electrochemical separation. Here, we have shown the recent developments in the research area of adsorption, photocatalysis, and filtration using graphene and its derivative-based materials.

5.1. Filtration

Filtration removes pollutants from contaminated water using a membrane film. There are several methods for doing this, including microfiltration, nanofiltration, membrane distillation, reverse osmosis, and forward osmosis. All these processes are based on the simple principle of separation of different molecules of either different sizes or different charges. The effectiveness of all these processes depends upon the type of membrane used for filtration. Pristine graphene and graphene oxide have come out as excellent membranes for filtration processes [146]. Graphene membranes can be used for nanofiltration, membrane distillation, reverse osmosis, and forward osmosis. The biggest advantage of graphene is its very small thickness, which directly affects the permeability of water through it. Pristine graphene on its own does not allow water to pass through it. The delocalized pi orbital on both sides of the graphene structure prohibits any material to pass through it, but this problem can be solved by creating pores on the graphene sheets [147]. These pores can be made in such a way that they will be large enough to let the water molecules pass through them, but which will hold back the other impurities. There are several methods for generating these holes. For example, exposing the graphene sheet to a gallium ion gun produces defects on the graphene sheets, and these sheets, when treated with an acidic solution, will form pores [147]. The size of these pores can be controlled by controlling the contact time of graphene with acid. Many researchers have been using various techniques to utilize this aspect of graphene for water and air filtration. For example, Vishwanath et al. used a multilayer graphene/cellulose composite for the filtration of methylene blue and Rose Bengal. The prepared composite showed that the filtration percentages for methylene blue and Rose Bengal were 98% and 94%, respectively [148]. Gayen et al. utilized graphene oxide in the filter bed for river water filtering and found a substantial difference in performance with and without the graphene filter. The iron removal efficiency was 84.5 and 70.7% with and without the graphene oxide filter. The removal effectiveness of hardness was 61.34% without a graphene oxide filter and 86.55% with one. Arsenic was removed 82% without graphene oxide and 90.9% with a graphene oxide filter. The fluoride removal efficiency was 58% without the graphene oxide filter and 73.1% with the graphene oxide filter [149]. Graphene shows promising results in the field of filtration. It can even be used in reverse osmosis for the filtration of saline water. Ndlwana et al. prepared mixed matrix membranes from polydopamine-crosslinked graphene nanoplatelets and found that the rejection of salts NaCl and $MgSO_4$ were enhanced to 99.85 and 99.95%, respectively, with the help of graphene [150]. All of these findings indicate that graphene will soon become an essential component of many filtration processes.

5.2. Adsorption

Adsorption has become a vital option for wastewater treatment in recent years. Low cost, reusability, high efficiency, high select ability, ease of use, wide pH range and high performance make adsorption one of the most likable processes for wastewater treatment. Adsorption can be used to remove organic or inorganic contaminants by chemical or physical adsorption [151]. Many adsorbents are currently being used for wastewater treatment such as activated carbon, starch, agriculture waste, cyclodextrins, zeolite, etc. [152]. Graphene as a novel material shows quite a promise in the field of adsorption for environmental applications such as wastewater treatment. Graphene shows high adsorption capacity because of its high surface area, high porosity, presence of a functional group, and the presence of π-π bonding. Graphene can either show chemical or physical adsorption. The type of adsorption can be determined by Dubinin–Radushkevich isotherms [153]. For example, Vasudevan and Lakshmi studied the adsorption of phosphane on graphene and by using Dubinin–Radushkevich isotherms, they found that adsorption was chemical by nature [154]. Zhu et al. showed the physical adsorption of CNCl and NH_3 on graphene due to the weaker adsorption energy and lower charge transfer [155]. Adsorption overall shows great potential for wastewater treatment such that many researchers have been developing various methods to enhance the adsorption capacity of graphene. For example, Dai et al. prepared polyvinyl alcohol-supported graphene oxide aerogel for wastewater treatment. The prepared sample showed that adsorption capacity was 96% for Congo red (CR) and methylene blue (MB), which were calculated using UV–Vis spectroscopy [156]. Nandi et al. prepared graphene nanoplatelets using human nails and obtained 99% adsorption of arsenic from wastewater [157]. Lingamdinne et al. prepared graphene oxide using the modified Hummer's method and they found that the maximum adsorption capacity for cobalt was 21.28 mg/g at pH 5.5 [158]. Azam et al. reported Hummer's synthesis of graphene oxide (GO) from graphite for the detoxification of Pb(II) from wastewater to control environmental pollution. The phenomenon of adsorption was taken into consideration for the removal of this toxic pollutant from the contaminated water. The possible mechanism followed by the GO adsorbent for the removal of heavy metal is explained in Figure 9 [159].

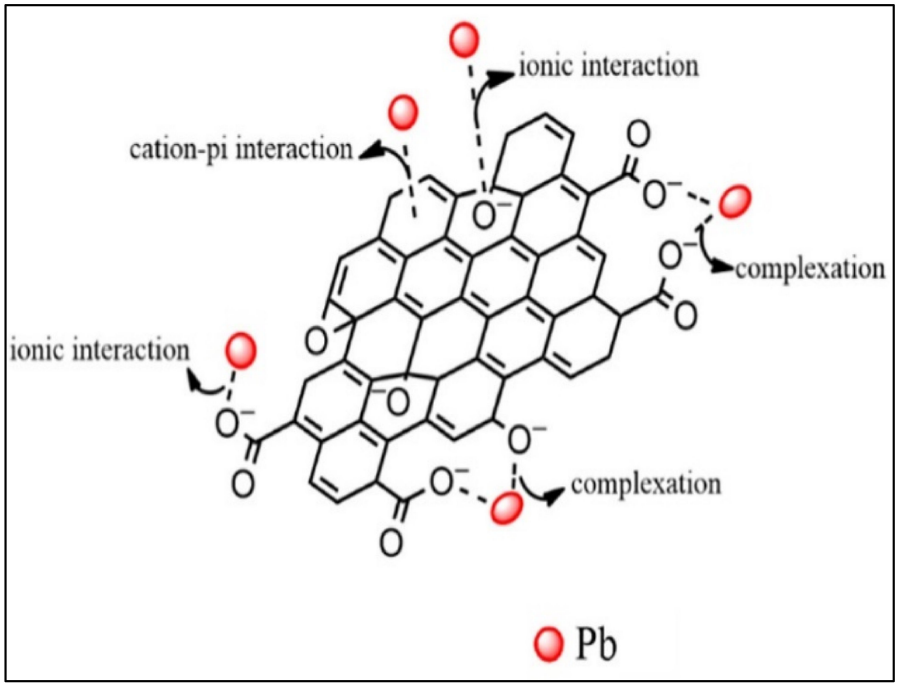

Figure 9. The probable adsorption mechanism of Pb(II) ions on the surface of graphene oxide from an aqueous solution (reprinted with permission from reference [159]).

5.3. Photocatalysis

Photocatalytic degradation is a type of advanced oxidation process. It has become a better approach to clean up wastewater because it can break down organic chemicals such as dyes that are difficult to break down using previous methods [160,161]. In order to degrade organic molecules via photocatalysis, you need a photocatalyst, which aids in the creation of radicals that further aid in the breakdown of organic compounds. When a photon with sufficient energy interacts with a photocatalyst, electrons move from the valence band to the conduction band. The valence band will develop a hole as a consequence of this action. After interacting with H_2O and O_2, the electron from the conduction band and the hole from the valence band may both contribute to the production of free radicals [162]. Because of their appropriate band gaps, semiconductors such as ZnO, TiO_2, ZnS, and MnO_2 are often used as photocatalysts. This is because their band gaps range from ~3.0 to 3.5 [163]. However, they have certain drawbacks such as low absorption rate of visible rays and fast recombination of electron and hole pairs generated during the process. This is the part where graphene can become a viable solution. Graphene's miraculous qualities including rapid electron transport, high electron acceptance (because of π-conjugation), high specific surface area, adsorption, mechanical strength, and chemical and thermal stability make it useful to be used with a semiconductor to increase their properties. Graphene porous structures with a higher number of trapping sites can hold semiconductors very firmly. Graphene can take electrons from these semiconductors, shortening the time required for electron–hole combination. It can also absorb visible light and transmit energy to the semiconductor, extending the range of spectra absorbed by the photocatalyst. A mechanism of the photocatalytic activity of graphene is shown in Figure 10.

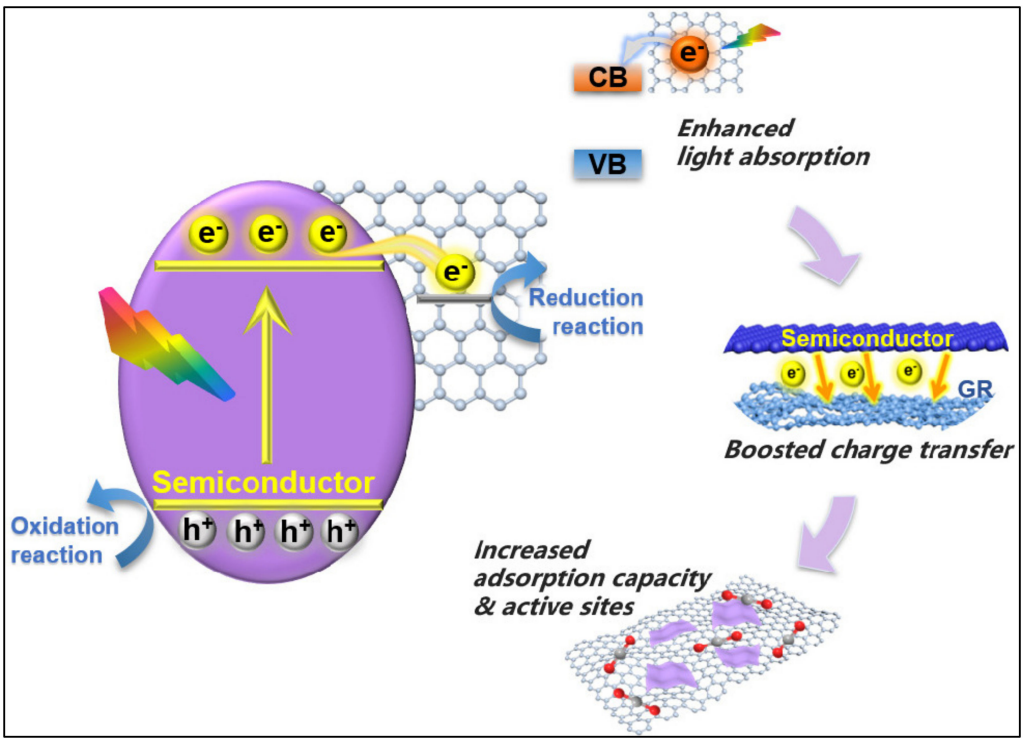

Figure 10. Graphene-based photocatalysis (reprinted with permission from [164]).

Researchers have developed graphene composites with different semiconductors to increase their performance; for example, Chen et al., (2021) found an increase in photocatalytic degradation of bisphenol A when they introduced the reduced graphene oxide in graphitic carbon nitride. This study shows how a promising metal-free rGO/g-C_3N_4 photocatalyst works to break down bisphenol A in visible light [165]. Israr et al., (2020) prepared a cobalt ferrite–graphene nanoplatelet-based composite. Their study showed

that the introduction of graphene increased the photocatalytic activity for the degradation of methylene blue from 38.3% to 98.7%. This was because graphene slowed down the recombination of electron–hole pairs in semiconductors [166]. Yan et al., (2020) prepared a graphene/polypyrrole composite and obtained a 94.8% removal efficiency of phenol using photocatalytic degradation [167]. Muhmood et al. prepared a heterojunction of graphitic carbon nitride and red phosphorus showing traits similar to graphene. The prepared samples were used for photocatalytic degradation of coloured and non-coloured, toxic category III organic compounds. The Mott–Schottky study revealed that the composite possessed type-I heterojunction with an enhanced catalytic behaviour. The improvement in catalytic behaviour was due to the charge transfer between red phosphorus and graphitic carbon nitride through heterojunction. It was observed that under the influence of visible light, photogenerated electrons moved from the conduction band of graphitic carbon nitrate to the conduction band of red phosphorus because of the higher negative edge potential of the graphitic carbon nitrate. On the other hand, the holes generated during this process were not able to move freely because of the increased negativity of the valence band of red phosphorus versus graphitic carbon nitrate. This whole process resulted in a lower recombination rate of holes and electrons, which in turn enhanced the photocatalytic activity of the prepared samples (Figure 11) [168].

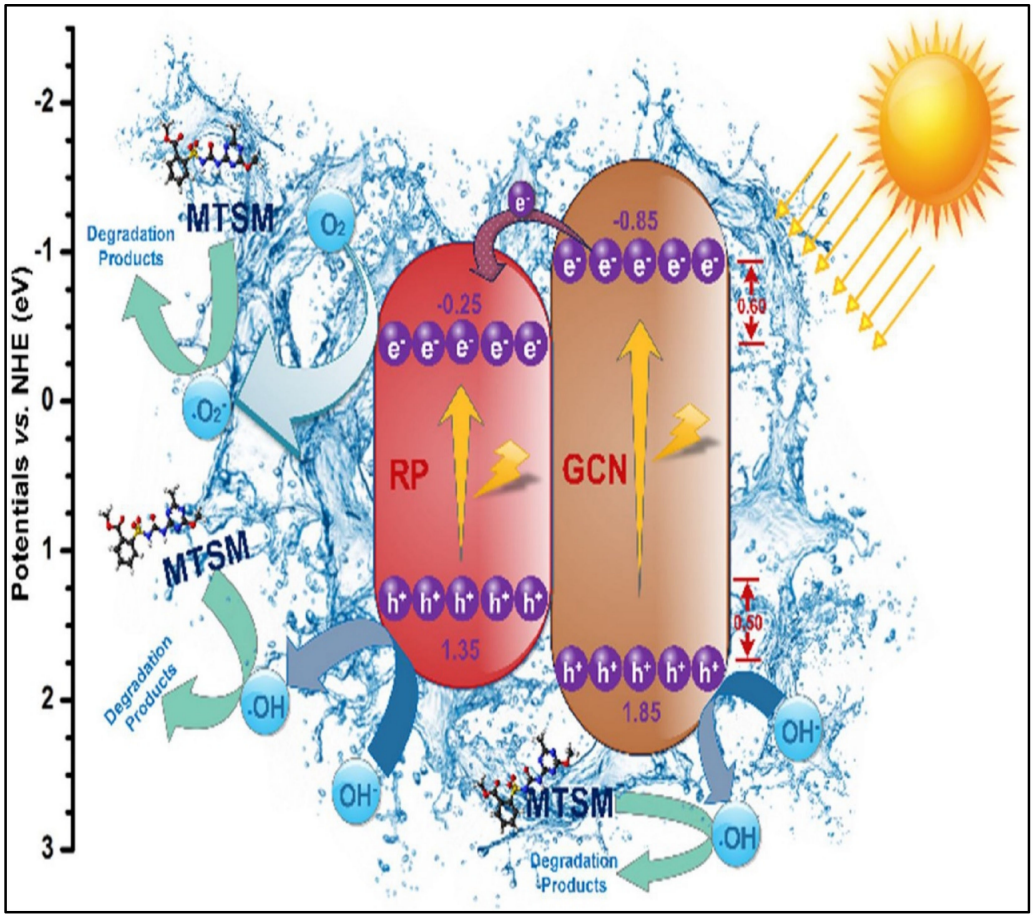

Figure 11. Schematic diagram of photo-generated charge transfer in red phosphorus/graphitic carbon nitride composite under visible light irradiation (reprinted with permission from reference [168]).

All these examples show that graphene can greatly enhance the photocatalytic ability of semiconductors, and graphene shows a promising future for environmental remediation due to its various abilities and properties. Table 4 summarizes numerous studies on wastewater treatment utilizing graphene and its composites. Furthermore, graphene shows antibacterial activity. Hu et al. in 2010 were the first ones to report the antibacterial

properties of graphene [169]. After that, many researchers studied the antibacterial and antimicrobial properties of graphene. Since then, other mechanisms for graphene antibacterial activity have been proposed, including oxidative stress, membrane stress, and electron transfer. When the graphene comes in contact with bacterial membranes, it can physically harm the bacterial productivity by deactivating their proteins and lipids. There is another way by which graphene can affect bacteria, and graphene electron acceptance can affect the integrity of the bacteria membrane by taking an electron from it. These recent studies have shown that graphene has the potential for antibacterial activity. Thus, graphene can provide an all-around solution for wastewater treatment [170].

Table 4. Graphene and its derivative-based composites for wastewater treatment.

Composite	Method	Pollutants	Efficiency	References
ZnO/RGO/Polyethylene glycole	Adsorption	Phenolic Pollutants	86.54% in 45 min	[171]
GO/Nitrogen-doped carbon	Adsorption	Uranium Pollutants	879.2 mg/g	[172]
rGO/CNT	Adsorptive filtration	Sulfamethoxazole	98–93%	[173]
Red phosphorus/Graphene	Photocatalysis	Rhodamine B	100% in 3 min	[174]
GO/PAN, GO/PPy, GO/Psty	Adsorption	Actacid orange	9.65, 43.99, 21.10 mg/g	[175]
mrGO/BiOCl, mrGO/BiOCl/Ag	Photocatalysis assisted Adsorption	Tinidazole	24% and 94%	[176]
RmGO/Polyaniline	Adsorption	Moxifloxacin and Ofloxacin	27.33 and 47.7 mg/g	[177]
GO/glass fibre	Filtration	Oil/water emulsion	99.4% retention rate	[178]
rGO/titanate nanotube	Hybrid adsorption/photocatalysis	Methylene blue	99.8%	[179]
Ag nanowires/TiO_2 nanosheets/graphene	Photocatalysis	Methylene blue	71–100% (under optimal condition)	[180]
graphene/MgAl	Adsorption	Chromium (VI)	172.55 mg/g	[181]
TiO_2/graphene	Photocatalysis	Methyl orange	100% in 210 min	[182]
Ag/Ag_3PO_4/$BiVO_4$/RGO	Photocatalysis	Tetracycline	94.96% in 60 min	[183]
g-C_3N_4/graphene quantum dots	Photocatalysis	Oxytetracycline	80% in 120 min	[184]
MnO_2/graphene	Adsorption	Tetracycline	1798 mg/g	[185]

6. Major Challenges for Environmental Applications of Graphene and Its Derivative-Based Composites

Even though graphene has extraordinary properties, and it can enhance the efficiency of many materials, the production of graphene is still in its initial phase. The cost of producing quality and pure graphene is still high, and only a few methods of producing graphene have been commercialized. There are still many challenges which must be addressed to fully utilize graphene. It is still a challenge to produce large amounts of defect-free graphene with a consistent structure. The conventional methods used for preparing graphene, such as mechanical exfoliation, cannot be used on a bigger scale, and the method which can be used on a bigger scale such as the chemical vapor deposition method can result in structural defects when transferring the graphene from one substrate to another. One of the methods to prepare graphene is by making use of graphite oxides, which are mostly made by the Hummer method. Hummer methods can cause the release of toxic gases such as chlorine dioxide and nitrogen dioxide, which pose a threat to the environment [186]. One of the major drawbacks of graphene is the limitation in its production. Recent studies have also shown that graphene can show cytotoxic and genotoxic tendencies. It has been observed that graphene, when inhaled, can cause damage to our lung cells because of the sharp edges present in it. Graphene derivatives are dissolvable in water and various

solutions; thus, there is always a risk of aquatic pollution from the overconcentration of graphene in water bodies. Knowledge and information about the toxic impacts of graphene are still largely unknown [187,188]. There are still many setbacks for graphene which must be overcome before using graphene in an efficient way for environmental application. Graphene must become a better option than conventionally used materials by lowing its adverse effects on the environment. Only then can it overtake the other conventionally used materials for environmental applications. Some of the major challenges in the path of utilizing graphene can be summarized:

- High-cost requirement for synthesis of high-grade graphene;
- Availability of scientifically matured conventional materials;
- Difficult to produce on a larger scale with the same consistency;
- Introduction of defects while handling graphene can cause significant loss in its properties;
- Graphene and its derivatives show cytotoxic and genotoxic tendencies;
- Sharp edges of graphene can cause cellular damage in the human body.

7. Future Scope and Concluding Remarks

Graphene has emerged as a wonderful material with amazing properties, which makes its derivatives promising candidates for the future. They can be introduced in many materials as a composite and can enhance their properties. They can be used in medical areas, electrical devices, and even for construction purposes. They can also be used in DNA sequencing, OLEDs, field effect transistors, membrane filtration, energy storage, etc. [189]. Since 2010, there has been a continuous increase in the number of reported studies in the area of graphene-based materials. In the future, improvement in the production of graphene might be a key point for the commercial development of graphene. Prior to its widespread commercial application, graphene's environmental drawbacks must all be overcome. In addition, it is essential to identify the negative effects of graphene on human health as early as possible so that the solutions to this problem may be studied as early as possible. Although a large number of studies are being performed on enhancing the properties of graphene and its derivatives, there is still very little research performed on its toxicity. To take further steps in the development of graphene-based materials, we must first overcome these small hurdles so that graphene potential can be fully utilized. In our review work, we have covered the background, properties, synthesis, and composites of graphene and its derivatives with different compounds. The environmental concern of graphene and its derivatives were also addressed by various techniques such as adsorption, filtration, and photocatalysis. Lastly, we provided an overview of the challenges and opportunities in the development of graphene and its derivatives in this study. Thus, we have concluded that graphene and its derivatives can behave as a beneficial and excellent photocatalyst and adsorbent material for potential environmental applications.

Author Contributions: Conceptualization, R.J.; Writing—original draft, S.K., H., J.P., S., R.J. and R.V.; Writing—review and editing, A.V., R.J., S.K.G., A.K., M.A.M.K., S.M.A. and J.A. All authors have read and agreed to the published version of the manuscript.

Funding: This research received no external funding.

Data Availability Statement: Not applicable.

Conflicts of Interest: The authors declare no conflict of interest.

References

1. Lee, X.J.; Hiew, B.Y.Z.; Lai, K.C.; Lee, L.Y.; Gan, S.; Thangalazhy-Gopakumar, S.; Rigby, S. Review on Graphene and Its Derivatives: Synthesis Methods and Potential Industrial Implementation. *J. Taiwan Inst. Chem. Eng.* **2019**, *98*, 163–180. [CrossRef]
2. Acheson, E.G. Graphite: Its Formation and Manufacture. *J. Frankl. Inst.* **1899**, *147*, 475–486. [CrossRef]
3. Brodie, B.C. On the Atomic Weight of Graphite. *Philos. Trans. R. Soc. Lond.* **1859**, *149*, 249–259.
4. Hummers, W.S., Jr.; Offeman, R.E. Preparation of Graphitic Oxide. *J. Am. Chem. Soc.* **1958**, *80*, 1339. [CrossRef]
5. Chen, H.; Li, C.; Qu, L. Solution Electrochemical Approach to Functionalized Graphene: History, Progress and Challenges. *Carbon* **2018**, *140*, 41–56. [CrossRef]

6. Abergel, D.S.L.; Apalkov, V.; Berashevich, J.; Ziegler, K.; Chakraborty, T. Properties of Graphene: A Theoretical Perspective. *Adv. Phys.* **2010**, *59*, 261–482. [CrossRef]
7. Kuang, Y.; Lindsay, L.; Shi, S.; Wang, X.; Huang, B. Thermal Conductivity of Graphene Mediated by Strain and Size. *Int. J. Heat Mass Transf.* **2016**, *101*, 772–778. [CrossRef]
8. Zhang, F.; Yang, K.; Liu, G.; Chen, Y.; Wang, M.; Li, S.; Li, R. Recent Advances on Graphene: Synthesis, Properties, and Applications. *Compos. Part Appl. Sci. Manuf.* **2022**, *160*, 107051. [CrossRef]
9. Güler, Ö.; Bağcı, N. A Short Review on Mechanical Properties of Graphene Reinforced Metal Matrix Composites. *J. Mater. Res. Technol.* **2020**, *9*, 6808–6833. [CrossRef]
10. Sánchez-Arellano, A.; Pérez-Huerta, J.S.; Ariza-Flores, D.; Sustaita-Torres, I.A.; Madrigal-Melchor, J. Tailoring the Transmission and Absorption Spectra in a Graphene-Dielectric Multilayer System for Lorentzian Profile in the Chemical Potential. *Superlattices Microstruct.* **2019**, *130*, 68–75. [CrossRef]
11. Fernandes, J.A.; Anselmo, D.; Vasconcelos, M.S.; Mello, V.D.; Cottam, M.G. Transmission and Absorption Spectra of Light Waves on Graphene-Embedded Cylindrical Photonic Quasicrystals. *Opt. Mater.* **2022**, *132*, 112865. [CrossRef]
12. Basak, T.; Basak, T. Electro-Absorption Spectra of Magnetic States of Diamond Shaped Graphene Quantum Dots. *Mater. Today Proc.* **2020**, *26*, 2058–2061. [CrossRef]
13. Wimmenauer, C.; Scheller, J.; Fasbender, S.; Heinzel, T. Single-Particle Energy–and Optical Absorption–Spectra of Multilayer Graphene Quantum Dots. *Superlattices Microstruct.* **2019**, *132*, 106171. [CrossRef]
14. Kizuka, T.; Miyazawa, K.; Matsuura, D. Synthesis of Carbon Nanocapsules and Nanotubes Using Fe-Doped Fullerene Nanowhiskers. *J. Nanotechnol.* **2012**, *2012*, 613746. [CrossRef]
15. Hashmi, A.; Nayak, V.; Singh, K.R.; Jain, B.; Baid, M.; Alexis, F.; Singh, A.K. Potentialities of Graphene and Its Allied Derivatives to Combat against SARS-CoV-2 Infection. *Mater. Today Adv.* **2022**, *13*, 100208. [CrossRef]
16. Sofo, J.O.; Chaudhari, A.S.; Barber, G.D. Graphane: A Two-Dimensional Hydrocarbon. *Phys. Rev. B* **2007**, *75*, 153401.
17. Sahin, H.; Leenaerts, O.; Singh, S.K.; Peeters, F.M. GraphAne: From Synthesis to Applications. *arXiv* **2015**, arXiv:1502.05804.
18. Yang, Y.-E.; Yang, Y.-R.; Yan, X.-H. Universal Optical Properties of Graphane Nanoribbons: A First-Principles Study. *Phys. E Low-Dimens. Syst. Nanostruct.* **2012**, *44*, 1406–1409.
19. Nagarajan, V.; Chandiramouli, R. A Novel Approach for Detection of NO_2 and SO_2 Gas Molecules Using Graphane Nanosheet and Nanotubes-A Density Functional Application. *Diam. Relat. Mater.* **2018**, *85*, 53–62.
20. Pumera, M.; Sofer, Z. Towards Stoichiometric Analogues of Graphene: Graphane, Fluorographene, Graphol, Graphene Acid and Others. *Chem. Soc. Rev.* **2017**, *46*, 4450–4463. [CrossRef]
21. Feng, W.; Long, P.; Feng, Y.; Li, Y. Two-Dimensional Fluorinated Graphene: Synthesis, Structures, Properties and Applications. *Adv. Sci.* **2016**, *3*, 1500413. [CrossRef] [PubMed]
22. Hrubỳ, V.; Zdražil, L.; Dzíbelová, J.; Šedajová, V.; Bakandritsos, A.; Lazar, P.; Otyepka, M. Unveiling the True Band Gap of Fluorographene and Its Origins by Teaming Theory and Experiment. *Appl. Surf. Sci.* **2022**, *587*, 152839. [CrossRef]
23. Wei, C.-K.; Peng, H.-Y.; Tsai, Y.-C.; Chen, T.-C.; Yang, C.-M. Fluorographene Sensing Membrane in a Light-Addressable Potentiometric Sensor. *Ceram. Int.* **2019**, *45*, 9074–9081. [CrossRef]
24. Geim, A.K. Graphene Prehistory. *Phys. Scr.* **2012**, *2012*, 014003. [CrossRef]
25. Geim, A.K. Nobel Lecture: Random Walk to Graphene. *Rev. Mod. Phys.* **2011**, *83*, 851. [CrossRef]
26. Zhu, Y.; Murali, S.; Cai, W.; Li, X.; Suk, J.W.; Potts, J.R.; Ruoff, R.S. Graphene and Graphene Oxide: Synthesis, Properties, and Applications. *Adv. Mater.* **2010**, *22*, 3906–3924. [CrossRef]
27. Chung, C.; Kim, Y.-K.; Shin, D.; Ryoo, S.-R.; Hong, B.H.; Min, D.-H. Biomedical Applications of Graphene and Graphene Oxide. *Acc. Chem. Res.* **2013**, *46*, 2211–2224. [CrossRef]
28. Smith, A.T.; LaChance, A.M.; Zeng, S.; Liu, B.; Sun, L. Synthesis, Properties, and Applications of Graphene Oxide/Reduced Graphene Oxide and Their Nanocomposites. *Nano Mater. Sci.* **2019**, *1*, 31–47. [CrossRef]
29. Coroş, M.; Pogăcean, F.; Măgeruşan, L.; Socaci, C.; Pruneanu, S. A Brief Overview on Synthesis and Applications of Graphene and Graphene-Based Nanomaterials. *Front. Mater. Sci.* **2019**, *13*, 1123. [CrossRef]
30. Muhmood, T.; Xia, M.; Lei, W.; Wang, F.; Khan, M.A. Design of Graphene Nanoplatelet/Graphitic Carbon Nitride Heterojunctions by Vacuum Tube with Enhanced Photocatalytic and Electrochemical Response. *Eur. J. Inorg. Chem.* **2018**, *2018*, 1726–1732. [CrossRef]
31. Mahmood, A.; Muhmood, T.; Ahmad, F. Carbon Nanotubes Heterojunction with Graphene like Carbon Nitride for the Enhancement of Electrochemical and Photocatalytic Activity. *Mater. Chem. Phys.* **2022**, *278*, 125640. [CrossRef]
32. Zhang, J.; Liu, Q.; Ruan, Y.; Lin, S.; Wang, K.; Lu, H. Monolithic Crystalline Swelling of Graphite Oxide: A Bridge to Ultralarge Graphene Oxide with High Scalability. *Chem. Mater.* **2018**, *30*, 1888–1897. [CrossRef]
33. Yu, W.; Sisi, L.; Haiyan, Y.; Jie, L. Progress in the Functional Modification of Graphene/Graphene Oxide: A Review. *RSC Adv.* **2020**, *10*, 15328–15345. [CrossRef]
34. Wang, C.; Sun, X.; Zhu, X.; Sun, B. Synthesis of Graphene via In-Liquid Discharge Plasma: A Green, Novel Strategy and New Insight. *Colloid Interface Sci. Commun.* **2022**, *47*, 100605. [CrossRef]
35. Wang, C.; Sun, X.; Zhu, X.; Sun, B. Alcohol Addition Improves the Liquid-Phase Plasma Process for "Green" Reduction of Graphene Oxide. *Vacuum* **2022**, *205*, 111373. [CrossRef]
36. Kalita, G.; Jaisi, B.P.; Umeno, M. Effective Reduction and Doping of Graphene Oxide Films at Near-Room Temperature by Microwave-Excited Surface-Wave Plasma Process. *Diam. Relat. Mater.* **2022**, *126*, 109066. [CrossRef]

37. Chettri, P.; Tripathi, A.; Tiwari, A. Effect of Silver Nanoparticles on Electrical and Magnetic Properties of Reduced Graphene Oxide. *Mater. Res. Bull.* **2022**, *150*, 111752. [CrossRef]
38. Pei, S.; Cheng, H.-M. The Reduction of Graphene Oxide. *Carbon* **2012**, *50*, 3210–3228. [CrossRef]
39. Sharma, N.; Tomar, S.; Shkir, M.; Choubey, R.K.; Singh, A. Study of Optical and Electrical Properties of Graphene Oxide. *Mater. Today Proc.* **2021**, *36*, 730–735. [CrossRef]
40. Rowley-Neale, S.J.; Randviir, E.P.; Dena, A.S.A.; Banks, C.E. An Overview of Recent Applications of Reduced Graphene Oxide as a Basis of Electroanalytical Sensing Platforms. *Appl. Mater. Today* **2018**, *10*, 218–226. [CrossRef]
41. Tarcan, R.; Todor-Boer, O.; Petrovai, I.; Leordean, C.; Astilean, S.; Botiz, I. Reduced Graphene Oxide Today. *J. Mater. Chem. C* **2020**, *8*, 1198–1224. [CrossRef]
42. Sreeprasad, T.S.; Maliyekkal, S.M.; Lisha, K.P.; Pradeep, T. Reduced Graphene Oxide–Metal/Metal Oxide Composites: Facile Synthesis and Application in Water Purification. *J. Hazard. Mater.* **2011**, *186*, 921–931. [CrossRef]
43. Ciammaruchi, L.; Bellucci, L.; Castillo, G.C.; Sánchez, G.M.-D.; Liu, Q.; Tozzini, V.; Martorell, J. Water Splitting of Hydrogen Chemisorbed in Graphene Oxide Dynamically Evolves into a Graphane Lattice. *Carbon* **2019**, *153*, 234–241. [CrossRef]
44. Joshi, N.C.; Gururani, P. Advances of Graphene Oxide Based Nanocomposite Materials in the Treatment of Wastewater Containing Heavy Metal Ions and Dyes. *Curr. Res. Green Sustain. Chem.* **2022**, *5*, 100306. [CrossRef]
45. Colmiais, I.; Silva, V.; Borme, J.; Alpuim, P.; Mendes, P.M. Towards RF Graphene Devices: A Review. *FlatChem* **2022**, *35*, 100409. [CrossRef]
46. Donaldson, L. New Graphene Transistors Could Offer New High-Frequency Devices. *Mater. Today* **2014**, *9*, 421. [CrossRef]
47. Routray, K.L.; Saha, S.; Behera, D. Nanosized $CoFe_2O_4$-Graphene Nanoplatelets with Massive Dielectric Enhancement for High Frequency Device Application. *Mater. Sci. Eng. B* **2020**, *257*, 114548. [CrossRef]
48. Szkopek, T.; Martel, E. Suspended Graphene Electromechanical Switches for Energy Efficient Electronics. *Prog. Quantum Electron.* **2021**, *76*, 100315. [CrossRef]
49. Htwe, Y.Z.N.; Mariatti, M. Printed Graphene and Hybrid Conductive Inks for Flexible, Stretchable, and Wearable Electronics: Progress, Opportunities, and Challenges. *J. Sci. Adv. Mater. Devices* **2022**, *7*, 100435. [CrossRef]
50. Arshad, M.U.; Dutta, D.; Sin, Y.Y.; Hsiao, S.W.; Wu, C.Y.; Chang, B.K.; Dai, L.; Su, C.Y. Multi-Functionalized Fluorinated Graphene Composite Coating for Achieving Durable Electronics: Ultralow Corrosion Rate and High Electrical Insulating Passivation. *Carbon* **2022**, *195*, 141–153. [CrossRef]
51. Miao, Y.; Li, P.; Cheng, S.; Zhou, Q.; Cao, M.; Yi, J.; Zhang, H. Preparation of Multi-Axial Compressible 3D PVDF Nanofibre/Graphene Wearable Composites Sensor Sponge and Application of Integrated Sensor. *Sens. Actuators Phys.* **2022**, *342*, 113648. [CrossRef]
52. Shen, T.; Gong, A.; Chen, J.; Liu, C.; Liu, X.; Feng, Y.; Duan, S. An Investigation on Temperature Sensor of SDTMS Structure with Ag-ZnO/Graphene Cladding. *Opt. Laser Technol.* **2022**, *153*, 108275. [CrossRef]
53. Benjamin, S.R.; Junior, E.J.M.R. Graphene-Based electrochemical sensors for detection of environmental pollutants. *Curr. Opin. Environ. Sci. Health* **2022**, *29*, 100381. [CrossRef]
54. Yabaş, E.; Biçer, E.; Altındal, A. Novel Reduced Graphene Oxide/Zinc Phthalocyanine and Reduced Graphene Oxide/Cobalt Phthalocyanine Hybrids as High Sensitivity Room Temperature Volatile Organic Compound Gas Sensors. *J. Mol. Struct.* **2023**, *1271*, 134076. [CrossRef]
55. Yusof, N.M.; Ibrahim, S.; Rozali, S. Synthesis of Graphene Oxide-Cobalt Oxide Hybrid Materials for Gas Sensors Application. *Mater. Today Proc.* **2022**, *66*, 2680–2684. [CrossRef]
56. Wang, Y.; Chen, J.; Qin, H.; Chen, K.; Li, Z.; Chen, Y.; Li, J.; Hu, T.; Chen, S.; Qiao, Z. Stress-Assisted Design of Stiffened Graphene Electrode Structure toward Compact Energy Storage. *J. Energy Chem.* **2022**, *71*, 478–487. [CrossRef]
57. Liu, Z.; Navik, R.; Tan, H.; Xiang, Q.; Goto, M.; Ibarra, R.M.; Zhao, Y. Graphene-Based Materials Prepared by Supercritical Fluid Technology and Its Application in Energy Storage. *J. Supercrit. Fluids* **2022**, *188*, 105672. [CrossRef]
58. Kumar, R.; Samykano, M.; Ngui, W.K.; Pandey, A.K.; Kalidasan, B.; Kadirgama, K.; Tyagi, V.V. Investigation of Thermal Performance and Chemical Stability of Graphene Enhanced Phase Change Material for Thermal Energy Storage. *Phys. Chem. Earth Parts ABC* **2022**, *128*, 103250. [CrossRef]
59. Zhou, X.; Huang, X.; Qi, X.; Wu, S.; Xue, C.; Boey, F.Y.; Yan, Q.; Chen, P.; Zhang, H. In Situ Synthesis of Metal Nanoparticles on Single-Layer Graphene Oxide and Reduced Graphene Oxide Surfaces. *J. Phys. Chem. C* **2009**, *113*, 10842–10846. [CrossRef]
60. Huang, J.; Zhang, L.; Chen, B.; Ji, N.; Chen, F.; Zhang, Y.; Zhang, Z. Nanocomposites of Size-Controlled Gold Nanoparticles and Graphene Oxide: Formation and Applications in SERS and Catalysis. *Nanoscale* **2010**, *2*, 2733–2738. [CrossRef]
61. Marquardt, D.; Vollmer, C.; Thomann, R.; Steurer, P.; Mülhaupt, R.; Redel, E.; Janiak, C. The Use of Microwave Irradiation for the Easy Synthesis of Graphene-Supported Transition Metal Nanoparticles in Ionic Liquids. *Carbon* **2011**, *49*, 1326–1332. [CrossRef]
62. Akhavan, O.; Abdolahad, M.; Esfandiar, A.; Mohatashamifar, M. Photodegradation of Graphene Oxide Sheets by TiO_2 Nanoparticles after a Photocatalytic Reduction. *J. Phys. Chem. C* **2010**, *114*, 12955–12959. [CrossRef]
63. Chen, S.; Zhu, J.; Wu, X.; Han, Q.; Wang, X. Graphene Oxide- MnO_2 Nanocomposites for Supercapacitors. *ACS Nano* **2010**, *4*, 2822–2830. [CrossRef] [PubMed]
64. Yin, Z.; Wu, S.; Zhou, X.; Huang, X.; Zhang, Q.; Boey, F.; Zhang, H. Electrochemical Deposition of ZnO Nanorods on Transparent Reduced Graphene Oxide Electrodes for Hybrid Solar Cells. *Small* **2010**, *6*, 307–312. [CrossRef] [PubMed]
65. Zhang, Y.I.; Zhang, L.; Zhou, C. Review of Chemical Vapor Deposition of Graphene and Related Applications. *Acc. Chem. Res.* **2013**, *46*, 2329–2339. [CrossRef] [PubMed]

66. Pirzado, A.A.; Le Normand, F.; Romero, T.; Paszkiewicz, S.; Papaefthimiou, V.; Ihiawakrim, D.; Janowska, I. Few-Layer Graphene from Mechanical Exfoliation of Graphite-Based Materials: Structure-Dependent Characteristics. *ChemEngineering* **2019**, *3*, 37. [CrossRef]
67. Othman, N.H.; Alias, N.H.; Shahruddin, M.Z.; Marpani, F.; Aba, N.D. Synthesis Methods of Graphene. In *Graphene, Nanotubes and Quantum Dots-Based Nanotechnology*; Elsevier: Amsterdam, The Netherlands, 2022; pp. 19–42.
68. Saeed, M.; Alshammari, Y.; Majeed, S.A.; Al-Nasrallah, E. Chemical Vapour Deposition of Graphene—Synthesis, Characterisation, and Applications: A Review. *Molecules* **2020**, *25*, 3856. [CrossRef]
69. Diallo, T.M.; Aziziyan, M.R.; Arvinte, R.; Ares, R.; Fafard, S.; Boucherif, A. CVD Growth of High-Quality Graphene over Ge (100) by Annihilation of Thermal Pits. *Carbon* **2021**, *174*, 214–226. [CrossRef]
70. Ji, Z.; Lin, Q.; Huang, Z.; Chen, S.; Gong, P.; Sun, Z.; Shen, B. Enhanced Lubricity of CVD Diamond Films by In-Situ Synthetization of Top-Layered Graphene Sheets. *Carbon* **2021**, *184*, 680–688. [CrossRef]
71. Jin, L.; Zhao, C.; Gong, Z.; Pan, J.; Wei, W.; Wang, G.; Cui, Y. Hydrogen-Promoted Graphene Growth on Pt(111) via CVD Methods. *Surf. Interfaces* **2021**, *26*, 101383. [CrossRef]
72. Bahri, M.; Shi, B.; Djebbi, K.; Elaguech, M.A.; Zhou, D.; Ben Ali, M.; Tlili, C.; Wang, D. Toward Clean and Crackless Polymer-Assisted Transfer of CVD-Grown Graphene and Its Recent Advances in GFET-Based Biosensors. *Mater. Today Chem.* **2021**, *22*, 100578. [CrossRef]
73. Yi, M.; Shen, Z. A Review on Mechanical Exfoliation for the Scalable Production of Graphene. *J. Mater. Chem. A* **2015**, *3*, 11700–11715. [CrossRef]
74. Baqiya, M.A.; Nugraheni, A.Y.; Islamiyah, W.; Kurniawan, A.F.; Ramli, M.M.; Yamaguchi, S.; Furukawa, Y.; Soontaranon, S.; Putra, E.G.R.; Cahyono, Y.; et al. Structural Study on Graphene-Based Particles Prepared from Old Coconut Shell by Acid–Assisted Mechanical Exfoliation. *Adv. Powder Technol.* **2020**, *31*, 2072–2078. [CrossRef]
75. Jayasena, B.; Melkote, S.N. An Investigation of PDMS Stamp Assisted Mechanical Exfoliation of Large Area Graphene. *Procedia Manuf.* **2015**, *1*, 840–853. [CrossRef]
76. Hayes, W.I.; Lubarsky, G.; Li, M.; Papakonstantinou, P. Mechanical Exfoliation of Graphite in 1-Butyl-3-Methylimidazolium Hexafluorophosphate (BMIM-PF6) Providing Graphene Nanoplatelets That Exhibit Enhanced Electrocatalysis. *J. Power Sources* **2014**, *271*, 312–325. [CrossRef]
77. Tiwari, S.K.; Kumar, V.; Huczko, A.; Oraon, R.; Adhikari, A.D.; Nayak, G.C. Magical Allotropes of Carbon: Prospects and Applications. *Crit. Rev. Solid State Mater. Sci.* **2016**, *41*, 257–317. [CrossRef]
78. Marcano, D.C.; Kosynkin, D.V.; Berlin, J.M.; Sinitskii, A.; Sun, Z.; Slesarev, A.; Alemany, L.B.; Lu, W.; Tour, J.M. Improved Synthesis of Graphene Oxide. *ACS Nano* **2010**, *4*, 4806–4814. [CrossRef]
79. Gebreegziabher, G.G.; Asemahegne, A.S.; Ayele, D.W.; Dhakshnamoorthy, M.; Kumar, A. One-Step Synthesis and Characterization of Reduced Graphene Oxide Using Chemical Exfoliation Method. *Mater. Today Chem.* **2019**, *12*, 233–239. [CrossRef]
80. Parvez, K.; Yang, S.; Feng, X.; Müllen, K. Exfoliation of Graphene via Wet Chemical Routes. *Synth. Met.* **2015**, *210*, 123–132. [CrossRef]
81. Das, P.; Zhang, L.; Zheng, S.; Shi, X.; Li, Y.; Wu, Z.-S. Rapid Fabrication of High-Quality Few-Layer Graphene through Gel-Phase Electrochemical Exfoliation of Graphite for High-Energy-Density Ionogel-Based Micro-Supercapacitors. *Carbon* **2022**, *196*, 203–212. [CrossRef]
82. Loudiki, A.; Matrouf, M.; Azriouil, M.; Farahi, A.; Lahrich, S.; Bakasse, M.; Mhammedi, M.A.E. Preparation of Graphene Samples via Electrochemical Exfoliation of Pencil Electrode: Physico-Electrochemical Characterization. *Appl. Surf. Sci. Adv.* **2022**, *7*, 100195. [CrossRef]
83. Alshamkhani, M.T.; Lahijani, P.; Lee, K.T.; Mohamed, A.R. Electrochemical Exfoliation of Graphene Using Dual Graphite Electrodes by Switching Voltage and Green Molten Salt Electrolyte. *Ceram. Int.* **2022**, *48*, 22534–22546. [CrossRef]
84. Pingale, A.D.; Owhal, A.; Katarkar, A.S.; Belgamwar, S.U.; Rathore, J.S. Facile Synthesis of Graphene by Ultrasonic-Assisted Electrochemical Exfoliation of Graphite. *Mater. Today Proc.* **2021**, *44*, 467–472. [CrossRef]
85. Gao, M.; Pan, Y.; Huang, L.; Hu, H.; Zhang, L.Z.; Guo, H.M.; Du, S.X.; Gao, H.-J. Epitaxial Growth and Structural Property of Graphene on Pt (111). *Appl. Phys. Lett.* **2011**, *98*, 033101. [CrossRef]
86. Liu, Z.; Xu, Q.; Zhang, C.; Sun, Q.; Wang, C.; Dong, M.; Wang, Z.; Ohmori, H.; Kosinova, M.; Goto, T.; et al. Laser-Induced Growth of Large-Area Epitaxial Graphene with Low Sheet Resistance on 4H-SiC(0001). *Appl. Surf. Sci.* **2020**, *514*, 145938. [CrossRef]
87. Deng, B.; Xin, Z.; Xue, R.; Zhang, S.; Xu, X.; Gao, J.; Tang, J.; Qi, Y.; Wang, Y.; Zhao, Y.; et al. Scalable and Ultrafast Epitaxial Growth of Single-Crystal Graphene Wafers for Electrically Tunable Liquid-Crystal Microlens Arrays. *Sci. Bull.* **2019**, *64*, 659–668. [CrossRef]
88. Xu, M.; Liang, T.; Shi, M.; Chen, H. Graphene-like Two-Dimensional Materials. *Chem. Rev.* **2013**, *113*, 3766–3798. [CrossRef]
89. Fan, Z.-J.; Yan, J.; Wei, T.; Ning, G.-Q.; Zhi, L.-J.; Liu, J.-C.; Cao, D.-X.; Wang, G.-L.; Wei, F. Nanographene-Constructed Carbon Nanofibers Grown on Graphene Sheets by Chemical Vapor Deposition: High-Performance Anode Materials for Lithium Ion Batteries. *ACS Nano* **2011**, *5*, 2787–2794. [CrossRef]
90. Yang, S.; Lohe, M.R.; Müllen, K.; Feng, X. New-Generation Graphene from Electrochemical Approaches: Production and Applications. *Adv. Mater.* **2016**, *28*, 6213–6221. [CrossRef]
91. Leenaerts, O.; Peelaers, H.; Hernández-Nieves, A.D.; Partoens, B.; Peeters, F.M. First-Principles Investigation of Graphene Fluoride and Graphane. *Phys. Rev. B* **2010**, *82*, 195436. [CrossRef]
92. Hu, J.Q.; Zhang, J.H.; Wu, S.Q.; Zhu, Z.Z. Hybrid Functional Studies on the Optical and Electronic Properties of Graphane and Silicane. *Solid State Commun.* **2015**, *209–210*, 59–65. [CrossRef]
93. Peng, Q.; Chen, Z.; De, S. A Density Functional Theory Study of the Mechanical Properties of Graphane With van Der Waals Corrections. *Mech. Adv. Mater. Struct.* **2015**, *22*, 717–721. [CrossRef]

94. Şahin, H.; Ataca, C.; Ciraci, S. Electronic and Magnetic Properties of Graphane Nanoribbons. *Phys. Rev. B* **2010**, *81*, 205417. [CrossRef]
95. Şahin, H.; Cahangirov, S.; Topsakal, M.; Bekaroglu, E.; Akturk, E.; Senger, R.T.; Ciraci, S. Monolayer Honeycomb Structures of Group-IV Elements and III-V Binary Compounds: First-Principles Calculations. *Phys. Rev. B* **2009**, *80*, 155453. [CrossRef]
96. Wei, W.; Jacob, T. Strong Many-Body Effects in Silicene-Based Structures. *Phys. Rev. B* **2013**, *88*, 045203. [CrossRef]
97. Şahin, H.; Topsakal, M.; Ciraci, S. Structures of Fluorinated Graphene and Their Signatures. *Phys. Rev. B* **2011**, *83*, 115432. [CrossRef]
98. Liu, H.Y.; Hou, Z.F.; Hu, C.H.; Yang, Y.; Zhu, Z.Z. Electronic and Magnetic Properties of Fluorinated Graphene with Different Coverage of Fluorine. *J. Phys. Chem. C* **2012**, *116*, 18193–18201. [CrossRef]
99. Klintenberg, M.; Lebègue, S.; Katsnelson, M.I.; Eriksson, O. Theoretical Analysis of the Chemical Bonding and Electronic Structure of Graphene Interacting with Group IA and Group VIIA Elements. *Phys. Rev. B* **2010**, *81*, 085433. [CrossRef]
100. Hernández Rosas, J.J.; Ramírez Gutiérrez, R.E.; Escobedo-Morales, A.; Chigo Anota, E. First Principles Calculations of the Electronic and Chemical Properties of Graphene, Graphane, and Graphene Oxide. *J. Mol. Model.* **2011**, *17*, 1133–1139. [CrossRef]
101. Papageorgiou, D.G.; Kinloch, I.A.; Young, R.J. Mechanical Properties of Graphene and Graphene-Based Nanocomposites. *Prog. Mater. Sci.* **2017**, *90*, 75–127. [CrossRef]
102. Cao, G. Atomistic Studies of Mechanical Properties of Graphene. *Polymers* **2014**, *6*, 2404–2432. [CrossRef]
103. Frank, I.W.; Tanenbaum, D.M.; van der Zande, A.M.; McEuen, P.L. Mechanical Properties of Suspended Graphene Sheets. *J. Vac. Sci. Technol. B Microelectron. Nanometer Struct. Process. Meas. Phenom.* **2007**, *25*, 2558–2561. [CrossRef]
104. Lee, C.; Wei, X.; Kysar, J.W.; Hone, J. Measurement of the Elastic Properties and Intrinsic Strength of Monolayer Graphene. *Science* **2008**, *321*, 385–388. [CrossRef] [PubMed]
105. Zhang, Y.; Pan, C. Measurements of Mechanical Properties and Number of Layers of Graphene from Nano-Indentation. *Diam. Relat. Mater.* **2012**, *24*, 1–5. [CrossRef]
106. Peng, Q.; Liang, C.; Ji, W.; De, S. A Theoretical Analysis of the Effect of the Hydrogenation of Graphene to Graphane on Its Mechanical Properties. *Phys. Chem. Chem. Phys.* **2013**, *15*, 2003–2011. [CrossRef]
107. Two-Dimensional Fluorinated Graphene: Synthesis, Structures, Properties and Applications-Feng-2016-Advanced Science-Wiley Online Library. Available online: https://onlinelibrary.wiley.com/doi/10.1002/advs.201500413 (accessed on 27 September 2022).
108. Liu, L.; Zhang, J.; Zhao, J.; Liu, F. Mechanical Properties of Graphene Oxides. *Nanoscale* **2012**, *4*, 5910–5916. [CrossRef]
109. Kang, S.-H.; Fang, T.-H.; Hong, Z.-H. Electrical and Mechanical Properties of Graphene Oxide on Flexible Substrate. *J. Phys. Chem. Solids* **2013**, *74*, 1783–1793. [CrossRef]
110. Sahin, H.; Leenaerts, O.; Singh, S.K.; Peeters, F.M. Graphane. *WIREs Comput. Mol. Sci.* **2015**, *5*, 255–272. [CrossRef]
111. Robinson, J.T.; Burgess, J.S.; Junkermeier, C.E.; Badescu, S.C.; Reinecke, T.L.; Perkins, F.K.; Zalalutdniov, M.K.; Baldwin, J.W.; Culbertson, J.C.; Sheehan, P.E.; et al. Properties of Fluorinated Graphene Films. *Nano Lett.* **2010**, *10*, 3001–3005. [CrossRef]
112. Jeon, K.-J.; Lee, Z.; Pollak, E.; Moreschini, L.; Bostwick, A.; Park, C.-M.; Mendelsberg, R.; Radmilovic, V.; Kostecki, R.; Richardson, T.J.; et al. Fluorographene: A Wide Bandgap Semiconductor with Ultraviolet Luminescence. *ACS Nano* **2011**, *5*, 1042–1046. [CrossRef]
113. Nair, R.R.; Ren, W.; Jalil, R.; Riaz, I.; Kravets, V.G.; Britnell, L.; Blake, P.; Schedin, F.; Mayorov, A.S.; Yuan, S.; et al. Fluorographene: A Two-Dimensional Counterpart of Teflon. *Small* **2010**, *6*, 2877–2884. [CrossRef]
114. Zhao, F.-G.; Zhao, G.; Liu, X.-H.; Ge, C.-W.; Wang, J.-T.; Li, B.-L.; Wang, Q.-G.; Li, W.-S.; Chen, Q.-Y. Fluorinated Graphene: Facile Solution Preparation and Tailorable Properties by Fluorine-Content Tuning. *J. Mater. Chem. A* **2014**, *2*, 8782–8789. [CrossRef]
115. Karlicky, F.; Otyepka, M. Band Gaps and Optical Spectra of Chlorographene, Fluorographene and Graphane from G0W0, GW0 and GW Calculations on Top of PBE and HSE06 Orbitals. *J. Chem. Theory Comput.* **2013**, *9*, 4155–4164. [CrossRef] [PubMed]
116. Rattana; Chaiyakun, S.; Witit-anun, N.; Nuntawong, N.; Chindaudom, P.; Oaew, S.; Kedkeaw, C.; Limsuwan, P. Preparation and Characterization of Graphene Oxide Nanosheets. *Procedia Eng.* **2012**, *32*, 759–764. [CrossRef]
117. Goumri, M.; Venturini, J.W.; Bakour, A.; Khenfouch, M.; Baitoul, M. Tuning the Luminescence and Optical Properties of Graphene Oxide and Reduced Graphene Oxide Functionnalized with PVA. *Appl. Phys. A* **2016**, *122*, 212. [CrossRef]
118. Qu, H.; Huang, L.; Han, Z.; Wang, Y.; Zhang, Z.; Wang, Y.; Chang, Q.; Wei, N.; Kipper, M.J.; Tang, J. A Review of Graphene-Oxide/Metal–Organic Framework Composites Materials: Characteristics, Preparation and Applications. *J. Porous Mater.* **2021**, *28*, 1837–1865. [CrossRef]
119. Zheng, Y.; Zheng, S.; Xue, H.; Pang, H. Metal-Organic Frameworks/Graphene-Based Materials: Preparations and Applications. *Adv. Funct. Mater.* **2018**, *28*, 1804950. [CrossRef]
120. Wang, Z.; Huang, J.; Mao, J.; Guo, Q.; Chen, Z.; Lai, Y. Metal–Organic Frameworks and Their Derivatives with Graphene Composites: Preparation and Applications in Electrocatalysis and Photocatalysis. *J. Mater. Chem. A* **2020**, *8*, 2934–2961. [CrossRef]
121. Li, S.; Tian, X.; Wang, J.; Xia, S.; Ma, L.; Zhou, J.; Li, C.; Qin, Z.; Qu, S. Design and Synthesis of Core-Shell Structure 3D-Graphene/Fe_3O_4@N-C Composite Derived from Fe-MOF as Lightweight Microwave Absorber. *Diam. Relat. Mater.* **2022**, *124*, 108941. [CrossRef]
122. Liu, S.; Li, B.; Yang, H.; Zhou, Y.; Xu, X.; Li, J. MOF-Derived Carbon/N-Doped Three Dimensional Reduced Graphene Oxide Composite with High Capacitive Deionization Performance. *Mater. Today Sustain.* **2022**, *20*, 100228. [CrossRef]
123. Mi, X.; Li, X. Construction of a Stable Porous Composite with Tunable Graphene Oxide in Ce-Based-MOFs for Enhanced Solar-Photocatalytic Degradation of Sulfamethoxazole in Water. *Sep. Purif. Technol.* **2022**, *301*, 122006. [CrossRef]
124. Bai, Y.-W.; Shi, G.; Gao, J.; Shi, F.-N. Synthesis, Crystal Structure of a Iron-Manganese Bimetal MOF and Its Graphene Composites with Enhanced Microwave Absorption Properties. *J. Phys. Chem. Solids* **2021**, *148*, 109657. [CrossRef]

125. Tang, B.; Dai, Y.; Sun, Y.; Chen, H.; Wang, Z. Graphene and MOFs Co-Modified Composites for High Adsorption Capacity and Photocatalytic Performance to Remove Pollutant under Both UV- and Visible-Light Irradiation. *J. Solid State Chem.* **2020**, *284*, 121215. [CrossRef]
126. Yang, M.-Q.; Zhang, N.; Pagliaro, M.; Xu, Y.-J. Artificial Photosynthesis over Graphene–Semiconductor Composites. Are We Getting Better? *Chem. Soc. Rev.* **2014**, *43*, 8240–8254. [CrossRef] [PubMed]
127. Muhmood, T.; Cai, Z.; Lin, S.; Xiao, J.; Hu, X.; Ahmad, F. Graphene/Graphitic Carbon Nitride Decorated with AgBr to Boost Photoelectrochemical Performance with Enhanced Catalytic Ability. *Nanotechnology* **2020**, *31*, 505602. [CrossRef] [PubMed]
128. Muhmood, T.; Uddin, A. Fabrication of Spherical-Graphitic Carbon Nitride via Hydrothermal Method for Enhanced Photo-Degradation Ability towards Antibiotic. *Chem. Phys. Lett.* **2020**, *753*, 137604. [CrossRef]
129. Lu, K.-Q.; Chen, Y.; Xin, X.; Xu, Y.-J. Rational Utilization of Highly Conductive, Commercial Elicarb Graphene to Advance the Graphene-Semiconductor Composite Photocatalysis. *Appl. Catal. B Environ.* **2018**, *224*, 424–432. [CrossRef]
130. Serry, M.; Sakr, M.A. Graphene-Metal-Semiconductor Composite Structure for Multimodal Energy Conversion. *Sens. Actuators Phys.* **2016**, *245*, 169–179. [CrossRef]
131. Chen, Y.; Zhai, B.; Liang, Y. Enhanced Degradation Performance of Organic Dyes Removal by Semiconductor/MOF/Graphene Oxide Composites under Visible Light Irradiation. *Diam. Relat. Mater.* **2019**, *98*, 107508. [CrossRef]
132. Dash, T.; Bihari Palei, B.; Dash, B.; Kumar Sahu, R.; Kumar Moharana, R.; Dhar, S.; Kumar Biswal, S. Graphene Reinforced Silicon Composites and Their Characterizations. *Mater. Today Proc.* **2022**, *62*, 5962–5964. [CrossRef]
133. Mallik, A.; Roy, I.; Chalapathi, D.; Narayana, C.; Das, T.D.; Bhattacharya, A.; Bera, S.; Bhattacharya, S.; De, S.; Das, B.; et al. Single Step Synthesis of Reduced Graphene Oxide/SnO_2 Nanocomposites for Potential Optical and Semiconductor Applications. *Mater. Sci. Eng. B* **2021**, *264*, 114938. [CrossRef]
134. Saran, N.; Thomas, T.L.; Bhavana, P. Dioxygen Reduction Using Electrochemically Reduced Graphene Oxide-Polymerized Cobalt-4-Pyridylporphyrin Composite. *Int. J. Hydrog. Energy* **2022**, *47*, 13629–13640. [CrossRef]
135. Hamidinejad, M.; Salari, M.; Ma, L.; Moghimian, N.; Zhao, B.; Taylor, H.K.; Filleter, T.; Park, C.B. Electrically and Thermally Graded Microcellular Polymer/Graphene Nanoplatelet Composite Foams and Their EMI Shielding Properties. *Carbon* **2022**, *187*, 153–164. [CrossRef]
136. Yao, L.; Liu, J.; Eedugurala, N.; Mahalingavelar, P.; Adams, D.J.; Wang, K.; Mayer, K.S.; Azoulay, J.D.; Ng, T.N. Ultrafast High-Energy Micro-Supercapacitors Based on Open-Shell Polymer-Graphene Composites. *Cell Rep. Phys. Sci.* **2022**, *3*, 100792. [CrossRef]
137. Oni, B.A.; Sanni, S.E. Cationic Graphene-Based Polymer Composite Modified with Chromium-Based Metal-Organic Framework [GP/MIL-53(Cr)] for the Degradation of 2,4-Dichlorophenol in Aqueous Solution. *Mater. Today Sustain.* **2022**, *18*, 100134. [CrossRef]
138. Gong, L.; Zhang, F.; Peng, X.; Scarpa, F.; Huang, Z.; Tao, G.; Liu, H.-Y.; Zhou, H.; Zhou, H. Improving the Damping Properties of Carbon Fiber Reinforced Polymer Composites by Interfacial Sliding of Oriented Multilayer Graphene Oxide. *Compos. Sci. Technol.* **2022**, *224*, 109309. [CrossRef]
139. Zhang, Y.; Wei, L.; Liu, X.; Ma, W.; Lou, C.; Wang, J.; Fan, S. Nanocellulose/N, O Co-Doped Graphene Composite Hydrogels for High Gravimetric and Volumetric Performance Symmetric Supercapacitors. *Int. J. Hydrog. Energy* **2022**, *47*, 33827–33838. [CrossRef]
140. Noureen, L.; Xie, Z.; Hussain, M.; Li, M.; Lyu, Q.; Wang, K.; Zhang, L.; Zhu, J. $BiVO_4$ and Reduced Graphene Oxide Composite Hydrogels for Solar-Driven Steam Generation and Decontamination of Polluted Water. *Sol. Energy Mater. Sol. Cells* **2021**, *222*, 110952. [CrossRef]
141. Wang, J.; Guo, Z.; Xiao, B.; Xiong, X.; Liu, G.; Wang, X. Reduced Graphene Oxide/$Cu_{7.2}S_4$ Composite Hydrogels for Highly Efficient Solar Steam Generation. *Mater. Today Sustain.* **2022**, *18*, 100121. [CrossRef]
142. Fong, K.K.; Tan, I.S.; Foo, H.C.Y.; Lam, M.K.; Tiong, A.C.Y.; Lim, S. Optimization and Evaluation of Reduced Graphene Oxide Hydrogel Composite as a Demulsifier for Heavy Crude Oil-in-Water Emulsion. *Chin. J. Chem. Eng.* **2021**, *33*, 297–305. [CrossRef]
143. Meng, Q.; Du, C.; Xu, Z.; Nie, J.; Hong, M.; Zhang, X.; Chen, J. Siloxene-Reduced Graphene Oxide Composite Hydrogel for Supercapacitors. *Chem. Eng. J.* **2020**, *393*, 124684. [CrossRef]
144. Saba, N.; Jawaid, M. Energy and Environmental Applications of Graphene and Its Derivatives. In *Polymer-Based Nanocomposites for Energy and Environmental Applications*; Elsevier: Amsterdam, The Netherlands, 2018; pp. 105–129.
145. Perreault, F.; de Faria, A.F.; Elimelech, M. Environmental Applications of Graphene-Based Nanomaterials. *Chem. Soc. Rev.* **2015**, *44*, 5861–5896. [CrossRef] [PubMed]
146. Aghigh, A.; Alizadeh, V.; Wong, H.Y.; Islam, M.S.; Amin, N.; Zaman, M. Recent Advances in Utilization of Graphene for Filtration and Desalination of Water: A Review. *Desalination* **2015**, *365*, 389–397. [CrossRef]
147. Ge, X.; Su, G.; Che, W.; Yang, J.; Zhou, X.; Wang, Z.; Qu, Y.; Yao, T.; Liu, W.; Wu, Y. Atomic Filtration by Graphene Oxide Membranes to Access Atomically Dispersed Single Atom Catalysts. *ACS Catal.* **2020**, *10*, 10468–10475. [CrossRef]
148. Vishwanath, H.S.; Shilpa, M.P.; Gurumurthy, S.C.; Gedda, M.; Ramam, K.; Eshwarappa, K.M.; Kirana, R.; Mishra, N.N.; Mundinamani, S. Flexible, Large-Area, Multi-Layered Graphene/Cellulose Composite for Dye Filtration Applications. *Mater. Today Commun.* **2022**, *30*, 103134. [CrossRef]
149. Gayen, S.; Bej, B.; Sankar Boxi, S.; Ghosh, R. Synthesis of Graphene Oxide and Its Application for Purification of River Water. *Mater. Today Proc.* **2022**, *in press*. [CrossRef]
150. Ndlwana, L.; Motsa, M.M.; Mamba, B.B. A Unique Method for Dopamine-Cross-Linked Graphene Nanoplatelets within Polyethersulfone Membranes (GNP-PDA/PES) for Enhanced Mechanochemical Resistance during NF and RO Desalination. *Eur. Polym. J.* **2020**, *136*, 109889. [CrossRef]

151. Kong, L.; Enders, A.; Rahman, T.S.; Dowben, P.A. Molecular Adsorption on Graphene. *J. Phys. Condens. Matter* **2014**, *26*, 443001. [CrossRef]
152. De Gisi, S.; Lofrano, G.; Grassi, M.; Notarnicola, M. Characteristics and Adsorption Capacities of Low-Cost Sorbents for Wastewater Treatment: A Review. *Sustain. Mater. Technol.* **2016**, *9*, 10–40. [CrossRef]
153. Sanyal, B.; Eriksson, O.; Jansson, U.; Grennberg, H. Molecular Adsorption in Graphene with Divacancy Defects. *Phys. Rev. B* **2009**, *79*, 113409. [CrossRef]
154. Vasudevan, S.; Lakshmi, J. The Adsorption of Phosphate by Graphene from Aqueous Solution. *RSC Adv.* **2012**, *2*, 5234–5242. [CrossRef]
155. Zhu, P.; Tang, F.; Wang, S.; Cao, W.; Wang, Q. Adsorption Performance of CNCl, NH_3 and GB on Modified Graphene and the Selectivity in O_2 and N_2 Environment. *Mater. Today Commun.* **2022**, *33*, 104280. [CrossRef]
156. Dai, J.; Huang, T.; Tian, S.; Xiao, Y.; Yang, J.; Zhang, N.; Wang, Y.; Zhou, Z. High Structure Stability and Outstanding Adsorption Performance of Graphene Oxide Aerogel Supported by Polyvinyl Alcohol for Waste Water Treatment. *Mater. Des.* **2016**, *107*, 187–197. [CrossRef]
157. Nandi, D.; Ghosh, S.K.; Ghosh, A.; Siengchin, S.; Roy, A.; Gupta, K.; Parameswaranpillai, J.; Bhowmick, A.K.; Ghosh, U.C. Arsenic Removal from Water by Graphene Nanoplatelets Prepared from Nail Waste: A Physicochemical Study of Adsorption Based on Process Optimization, Kinetics, Isotherm and Thermodynamics. *Environ. Nanotechnol. Monit. Manag.* **2021**, *16*, 100564. [CrossRef]
158. Lingamdinne, L.P.; Koduru, J.R.; Roh, H.; Choi, Y.-L.; Chang, Y.-Y.; Yang, J.-K. Adsorption Removal of Co(II) from Waste-Water Using Graphene Oxide. *Hydrometallurgy* **2016**, *165*, 90–96. [CrossRef]
159. Azam, M.G.; Kabir, M.H.; Shaikh, M.A.A.; Ahmed, S.; Mahmud, M.; Yasmin, S. A Rapid and Efficient Adsorptive Removal of Lead from Water Using Graphene Oxide Prepared from Waste Dry Cell Battery. *J. Water Process Eng.* **2022**, *46*, 102597. [CrossRef]
160. Rueda-Marquez, J.J.; Levchuk, I.; Fernández Ibañez, P.; Sillanpää, M. A Critical Review on Application of Photocatalysis for Toxicity Reduction of Real Wastewaters. *J. Clean. Prod.* **2020**, *258*, 120694. [CrossRef]
161. Li, F.; Cheng, L.; Fan, J.; Xiang, Q. Steering the Behavior of Photogenerated Carriers in Semiconductor Photocatalysts: A New Insight and Perspective. *J. Mater. Chem. A* **2021**, *9*, 23765–23782. [CrossRef]
162. Marinho, B.A.; Suhadolnik, L.; Likozar, B.; Huš, M.; Marinko, Ž.; Čeh, M. Photocatalytic, Electrocatalytic and Photoelectrocatalytic Degradation of Pharmaceuticals in Aqueous Media: Analytical Methods, Mechanisms, Simulations, Catalysts and Reactors. *J. Clean. Prod.* **2022**, *343*, 131061. [CrossRef]
163. Gopinath, K.P.; Madhav, N.V.; Krishnan, A.; Malolan, R.; Rangarajan, G. Present Applications of Titanium Dioxide for the Photocatalytic Removal of Pollutants from Water: A Review. *J. Environ. Manage.* **2020**, *270*, 110906. [CrossRef]
164. Li, Y.-H.; Tang, Z.-R.; Xu, Y.-J. Multifunctional Graphene-Based Composite Photocatalysts Oriented by Multifaced Roles of Graphene in Photocatalysis. *Chin. J. Catal.* **2022**, *43*, 708–730. [CrossRef]
165. Chen, Y.-H.; Wang, B.-K.; Hou, W.-C. Graphitic Carbon Nitride Embedded with Graphene Materials towards Photocatalysis of Bisphenol A: The Role of Graphene and Mediation of Superoxide and Singlet Oxygen. *Chemosphere* **2021**, *278*, 130334. [CrossRef] [PubMed]
166. Israr, M.; Iqbal, J.; Arshad, A.; Rani, M.; Gómez-Romero, P.; Benages, R. Graphene Triggered Enhancement in Visible-Light Active Photocatalysis as Well as in Energy Storage Capacity of $(CFO)_{1-x}(GNPs)_x$ Nanocomposites. *Ceram. Int.* **2020**, *46*, 2630–2639. [CrossRef]
167. Yan, S.; Song, H.; Li, Y.; Yang, J.; Jia, X.; Wang, S.; Yang, X. Integrated Reduced Graphene Oxide/Polypyrrole Hybrid Aerogels for Simultaneous Photocatalytic Decontamination and Water Evaporation. *Appl. Catal. B Environ.* **2022**, *301*, 120820. [CrossRef]
168. Muhmood, T.; Xia, M.; Lei, W.; Wang, F. Under Vacuum Synthesis of Type-I Heterojunction between Red Phosphorus and Graphene like Carbon Nitride with Enhanced Catalytic, Electrochemical and Charge Separation Ability for Photodegradation of an Acute Toxicity Category-III Compound. *Appl. Catal. B Environ.* **2018**, *238*, 568–575. [CrossRef]
169. Hu, W.; Peng, C.; Luo, W.; Lv, M.; Li, X.; Li, D.; Huang, Q.; Fan, C. Graphene-Based Antibacterial Paper. *ACS Nano* **2010**, *4*, 4317–4323. [CrossRef]
170. Kumar, P.; Huo, P.; Zhang, R.; Liu, B. Antibacterial Properties of Graphene-Based Nanomaterials. *Nanomaterials* **2019**, *9*, 737. [CrossRef]
171. Rout, D.R.; Jena, H.M. Polyethylene Glycol Functionalized Reduced Graphene Oxide Coupled with Zinc Oxide Composite Adsorbent for Removal of Phenolic Wastewater. *Environ. Res.* **2022**, *214*, 114044. [CrossRef]
172. Cao, M.; Chen, L.; Xu, W.; Gao, J.; Gui, Y.; Ma, F.; Liu, P.; Xue, Y.; Yan, Y. Preparation of Graphene Oxide Composite Nitrogen-Doped Carbon (GO@NCs) by One-Step Carbonization with Enhanced Electrosorption Performance for U(VI). *J. Water Process Eng.* **2022**, *48*, 102930. [CrossRef]
173. Sheng, J.; Yin, H.; Qian, F.; Huang, H.; Gao, S.; Wang, J. Reduced Graphene Oxide-Based Composite Membranes for in-Situ Catalytic Oxidation of Sulfamethoxazole Operated in Membrane Filtration. *Sep. Purif. Technol.* **2020**, *236*, 116275. [CrossRef]
174. Li, W.; Zhang, Y.; Tian, G.; Xie, S.; Xu, Q.; Wang, L.; Tian, J.; Bu, Y. Fabrication of Graphene-Modified Nano-Sized Red Phosphorus for Enhanced Photocatalytic Performance. *J. Mol. Catal. Chem.* **2016**, *423*, 356–364. [CrossRef]
175. Noreen, S.; Tahira, M.; Ghamkhar, M.; Hafiz, I.; Bhatti, H.N.; Nadeem, R.; Murtaza, M.A.; Yaseen, M.; Sheikh, A.A.; Naseem, Z.; et al. Treatment of Textile Wastewater Containing Acid Dye Using Novel Polymeric Graphene Oxide Nanocomposites (GO/PAN, GO/PPy, GO/PSty). *J. Mater. Res. Technol.* **2021**, *14*, 25–35. [CrossRef]
176. Sohani, S.; Ara, B.; Khan, H.; Gul, K.; Khan, M. Photocatalytic Assessed Adsorptive Removal of Tinidazole from Aqueous Environment Using Reduced Magnetic Graphene Oxide-Bismuth Oxychloride and Its Silver Composite. *Environ. Res.* **2022**, *215*, 114262. [CrossRef]
177. Ullah, T.; Gul, K.; Khan, H.; Ara, B.; Zia, T.U.H. Efficient Removal of Selected Fluoroquinolones from the Aqueous Environment Using Reduced Magnetic Graphene Oxide/Polyaniline Composite. *Chemosphere* **2022**, *293*, 133452. [CrossRef]

178. Xie, W.; Chen, M.; Wei, S.; Huang, Z.; Li, Z. Lignin Nanoparticles-Intercalated Reduced Graphene Oxide/Glass Fiber Composite Membranes for Highly Efficient Oil-in-Water Emulsions Separation in Harsh Environment. *Colloids Surf. Physicochem. Eng. Asp.* **2022**, *648*, 129190. [CrossRef]
179. Nguyen, C.H.; Juang, R.-S. Efficient Removal of Methylene Blue Dye by a Hybrid Adsorption–Photocatalysis Process Using Reduced Graphene Oxide/Titanate Nanotube Composites for Water Reuse. *J. Ind. Eng. Chem.* **2019**, *76*, 296–309. [CrossRef]
180. Liu, C.; Lin, Y.; Dong, Y.; Wu, Y.; Bao, Y.; Yan, H.; Ma, J. Fabrication and Investigation on Ag Nanowires/TiO_2 Nanosheets/Graphene Hybrid Nanocomposite and Its Water Treatment Performance. *Adv. Compos. Hybrid Mater.* **2020**, *3*, 402–414. [CrossRef]
181. Yuan, X.; Wang, Y.; Wang, J.; Zhou, C.; Tang, Q.; Rao, X. Calcined Graphene/MgAl-Layered Double Hydroxides for Enhanced Cr(VI) Removal. *Chem. Eng. J.* **2013**, *221*, 204–213. [CrossRef]
182. Chen, L.; Yang, S.; Mu, L.; Ma, P.-C. Three-Dimensional Titanium Dioxide/Graphene Hybrids with Improved Performance for Photocatalysis and Energy Storage. *J. Colloid Interface Sci.* **2018**, *512*, 647–656. [CrossRef]
183. Chen, F.; Yang, Q.; Li, X.; Zeng, G.; Wang, D.; Niu, C.; Zhao, J.; An, H.; Xie, T.; Deng, Y. Hierarchical Assembly of Graphene-Bridged Ag_3PO_4/Ag/$BiVO_4$ (040) Z-Scheme Photocatalyst: An Efficient, Sustainable and Heterogeneous Catalyst with Enhanced Visible-Light Photoactivity towards Tetracycline Degradation under Visible Light Irradiation. *Appl. Catal. B Environ.* **2017**, *200*, 330–342. [CrossRef]
184. Yuan, A.; Lei, H.; Xi, F.; Liu, J.; Qin, L.; Chen, Z.; Dong, X. Graphene Quantum Dots Decorated Graphitic Carbon Nitride Nanorods for Photocatalytic Removal of Antibiotics. *J. Colloid Interface Sci.* **2019**, *548*, 56–65. [CrossRef] [PubMed]
185. Song, Z.; Ma, Y.-L.; Li, C.-E. The Residual Tetracycline in Pharmaceutical Wastewater Was Effectively Removed by Using MnO_2/Graphene Nanocomposite. *Sci. Total Environ.* **2019**, *651*, 580–590. [CrossRef] [PubMed]
186. Short Review on the Use of Graphene as a Biomaterial –Prospects, and Challenges in Brazil. *J. Mater. Res. Technol.* **2022**, *19*, 2410–2430. [CrossRef]
187. Yan, Z.; Yang, X.; Lynch, I.; Cui, F. Comparative Evaluation of the Mechanisms of Toxicity of Graphene Oxide and Graphene Oxide Quantum Dots to Blue-Green Algae Microcystis Aeruginosa in the Aquatic Environment. *J. Hazard. Mater.* **2022**, *425*, 127898. [CrossRef]
188. Raja, I.S.; Molkenova, A.; Kang, M.S.; Lee, S.H.; Lee, J.E.; Kim, B.; Han, D.-W.; Atabaev, T.S. Differential Toxicity of Graphene Family Nanomaterials Concerning Morphology. In *Multifaceted Biomedical Applications of Graphene*; Springer: Berlin/Heidelberg, Germany, 2022; pp. 23–39.
189. Yue, X.; Fan, J.; Xiang, Q. Internal Electric Field on Steering Charge Migration: Modulations, Determinations and Energy-Related Applications. *Adv. Funct. Mater.* **2022**, *32*, 2110258. [CrossRef]